Optimal allocation of vaccines - the role of childrens' vaccination

Nir Gavish[1*], Guy Katriel[2]

[1]Faculty of Mathematics, Technion - IIT, Haifa, Israel

[2]Department of Applied Mathematics, ORT Braude College of Engineering, Karmiel, Israel

[*]To whom correspondence should be addressed; E-mail: ngavish@technion.ac.il

The ultimate goal of COVID-19 vaccination campaigns is to enable the return of societies and economies to a state of normality. Presently, vaccines have not been approved for children. In this work, we use mathematical modeling and optimization to study the effect of the ineligibility of children for vaccination on the effectiveness of a vaccination campaign. Particularly, we address the question of whether vaccination of children of age 10 and older, once approved, should be given higher priority than the vaccination of other age groups. We consider optimal allocations according to competing measures and systematically study the trade-offs among them. We find that, under all scenarios considered, optimal allocations of vaccines do not include age-group 0-9. In contrast, in many of these cases, optimal allocations of vaccines do include the age group 10-19, though the degree to which inclusion of this age group improves outcomes varies by case.

Introduction The availability of effective vaccines against SARS-CoV-19 is widely seen as a game-changer that will enable an eventual return to normal life in those countries in which

it becomes available, following the devastating COVID-19 pandemic. Presently no vaccine has been approved for children under 16, and current efforts are focused on extending vaccine approval for children above 12 (*1*). A key question is whether and to what extent the fact that children cannot be vaccinated will reduce the effectiveness of a vaccination campaign at the population level (*2, 3*). Children are, on the one hand, a relatively large age group that tend to interact more intensively than other age groups. On the other hand, it has been estimated that children's susceptibility to SARS-CoV-19 is significantly lower than that of adults (*4, 5*), so that children can be effectively viewed as if they are already vaccinated with a vaccine of partial efficacy.

In this work we present a mathematical model to explore the effect of demography, age-based social interaction structure, and vaccine efficacy on the optimal post-vaccination outcomes that can be achieved by a suitable allocation of vaccines, in the context of the COVID-19 pandemic. In particular, our study focuses on two questions:

1. What are the prospects for achieving herd immunity assuming vaccine allocation is performed optimally, and what are the age-dependent vaccine allocations which will achieve herd immunity with minimal vaccination coverage?

2. If herd immunity cannot be achieved, what are the optimal outcomes - according to different possible measures - that can be achieved, and what are the age-dependent vaccine allocations that will achieve them?

We consider outcomes in the medium-term range, after the vaccination campaign has ended. Our approach is useful for characterizing the optimal age-based allocation of vaccines that could result from a successful vaccination campaign. It does not, however, shed light on the design of the vaccination campaign, e.g., on the temporal prioritization of vaccines during the vaccination campaign. In this sense, our work is complementary to other works which focus on

the vaccination effort itself and its optimized design as it competes with the spread of infection (*6, 7*). Our work is also complementary to other works which consider the optimized allocation of COVID-19 vaccines, in that we address the issue of restrictions on the eligibility of children (*8, 9*).

Vaccination policies are commonly optimized to minimize a single measure such as mortality, infections, or hospitalizations (*6–10*). Here, we take a different approach and consider the problem as one of multi-objective optimization. Using this approach, we systematically evaluate the trade-offs between competing measures such as mortality and number of infections.

Our key findings can be summarized as follows:

- Vaccination of children in age group 10-19 is essential to achieve herd immunity via vaccination, unless vaccine coverage is very high. By contrast, in many cases, herd immunity at relevant values of R_0 can be reached without the vaccination of age group 0-9.

- Designing vaccine allocation with the aim of achieving herd immunity is not a robust strategy as it leaves the older age groups exposed, if, due to a misestimation or to changed circumstances, herd-immunity is not achieved.

- Vaccine allocations aimed at minimizing mortality are only marginally affected by the ineligibility of age groups 0-9 or 0-19. However, our results show that upon relaxing non-pharmaceutical interventions, mortality-minimizing allocations give rise to a large number of infections with a high attack rate in children.

- Optimal vaccine allocations that also give weight to the number of infections include age group 10-19. Consequently, ineligibility of age group 10-19 results in worse outcomes. On the other hand, age group 0-9 is not included in these optimal vaccine allocations. These results suggest that under the criteria studied, vaccination of age group 0-9 should not be of priority.

The results, as well as results in other settings, may be further explored using open-source and interactive tools that accompany this study. A case study using data from Israel, demonstrating the application of the tools developed in this work, is included in the supplementary material.

Assumptions on vaccine efficacy A full account of the assumptions used in this work is available in the supplementary material. Here, we highlight the assumptions regarding vaccine efficacy as they are central to the interpretation of the results. Unless otherwise specified, in what follows, we assume that the susceptibility of vaccinated individuals is reduced by 80%, and the risk of a vaccinated infectee to develop severe disease is 25% that of a non-vaccinated infectee. By construction, this combination of parameters gives rise to an overall reduction of 95% in the risk of a vaccinated individual to develop severe disease as estimated in controlled studies (*11*) and analysis of real-world data (*12*).

Can herd immunity be achieved? We consider scenarios of a partial return to normality, to a basic reproduction number of R_0, after vaccination efforts are completed. Note that R_0 denotes the reproductive number in the absence of vaccination and preexisting immunity due to recovery. For each value of R_0, we compute an *optimal* vaccine allocation among the eligible age groups, achieving herd immunity with a minimal fraction $V_{\text{threshold}}$ of the population vaccinated. See the supplementary material for details on these computations.

We first examine the case in which the entire population of the USA is eligible for vaccination. In this case, the optimal allocations prioritize different age groups in a way that varies with the reproductive number R_0. For example, when R_0 is less than ≈ 1.1, vaccine supply is allocated solely to age group 30-39, see Figure 1B. Then, as R_0 increases, vaccine supply is gradually extended to additional age groups. The optimal vaccine allocations are not necessarily allocations to those who do the most transmitting. Indeed, as R_0 increases, additional age groups are typically added to the allocation before the coverage of the age groups already

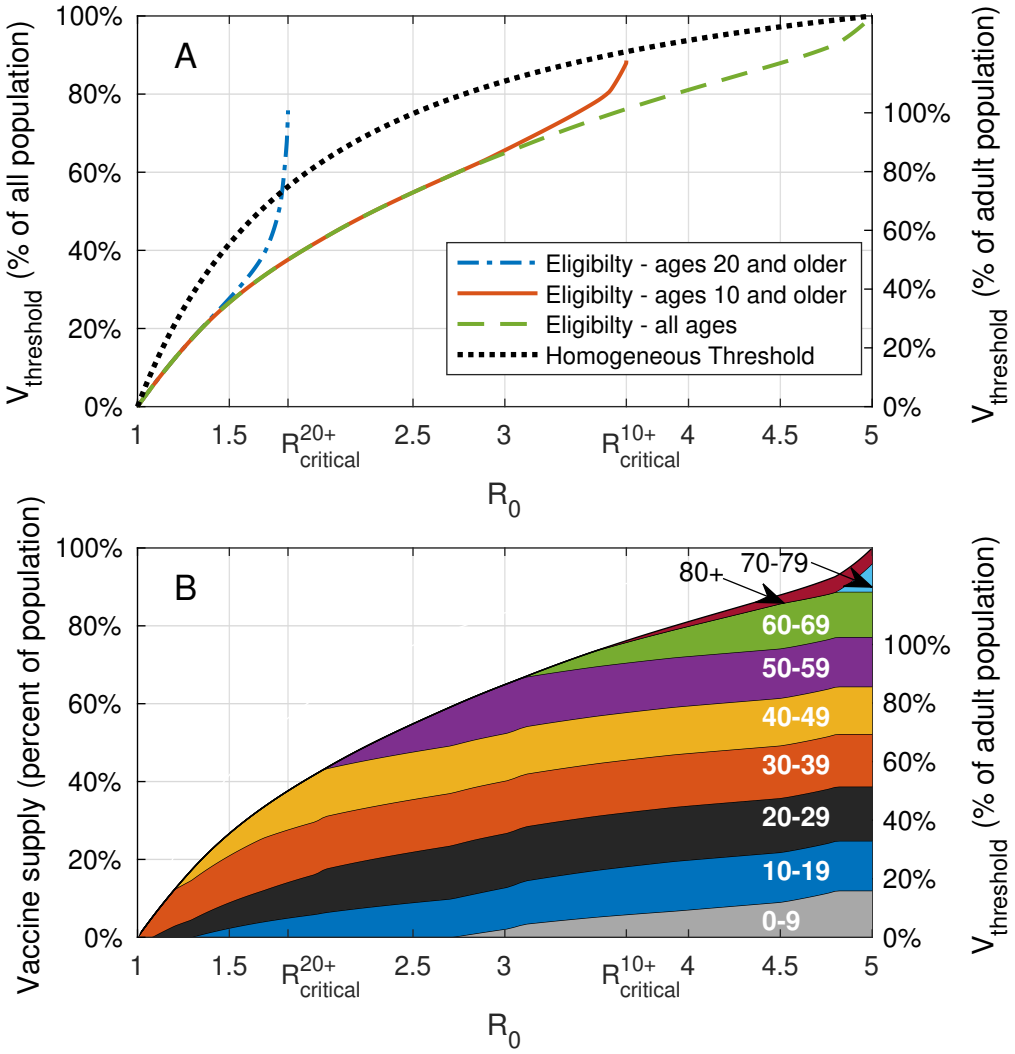

Figure 1: **Vaccination coverage required for herd immunity.** A: Vaccine coverage $V_{\text{threshold}}$ required to achieve herd immunity threshold as a function of the reproduction number R_0 for the USA demography and contact structure. B: Vaccine allocations at which herd immunity is achieved at minimal vaccine coverage and when all the population is eligible for vaccination.

present in the allocation has reached 100%. For $R_0 = 3$, herd immunity can be achieved by vaccinating roughly 65% of the population in an optimal way, see Figure 1A. In comparison, if vaccines are allocated *pro rata* (in proportion to the size of age groups), achieving herd immunity requires vaccination of 85% of the population, taking into account 80% vaccine efficacy

against infection.

In the case of vaccine eligibility for ages 10 and older, we observe that for low values of R_0 the threshold curve $V^{10+}_{\text{threshold}}$ coincides with the threshold curve $V_{\text{threshold}}$ corresponding to the case in which all ages are vaccine eligible. The reason for this is that for values of $R_0 < 2.5$, even when the vaccination of all age groups is allowed, the optimal allocation does not include the $0-9$ age group, see Figure 1B. For higher values of R_0, however, the two curves diverge and the threshold curve $V^{10+}_{\text{threshold}}$ rapidly increases up to its maximal value which corresponds to 100% of the eligible population at $R_0 = R^{10+}_{\text{critical}} \approx 3.6$. When $R_0 > R^{10+}_{\text{critical}}$, reaching herd immunity becomes impossible if children under the age of 10 are not vaccinated. In contrast, in the case of vaccine eligibility for ages 20 and older, we find that herd immunity is achievable only for rather low reproductive numbers, $R_0 < R^{20+}_{\text{critical}} \approx 1.8$. This means that for higher values of R_0, even if *all* adults over 20 were vaccinated, the spread of the infection would be sustained solely by the population under the age of 20. The above example, presented in Figure 1, relies on the demographic structure and the contact matrix of the USA. We have also examined the critical reproduction numbers $R^{10+}_{\text{critical}}$ and $R^{20+}_{\text{critical}}$ for eight additional countries and found the results to be similar, see Figure 2A. We further observe that the question of whether the infection can be eradicated without vaccinating children is not answered by looking at the percentage of children in the population, as a naive calculation based on a homogeneous-population model would imply. For example, in the case of Zimbabwe, with 53% of its population in age group 0-19, we computed $R^{20+}_{\text{critical}} \approx 2.05$, which is higher than $R^{20+}_{\text{critical}} \approx 1.8$ computed for Poland for which the size of age group 0-19 is 20% of the total population. Rather, the key factor is the level of assortativity of mixing within the children sub-population, as reflected in the contact matrix.

We find that the above results are quite insensitive to variations in assumptions concerning vaccine efficacy, vaccine hesitancy, or when considering the case of all-or-none rather than

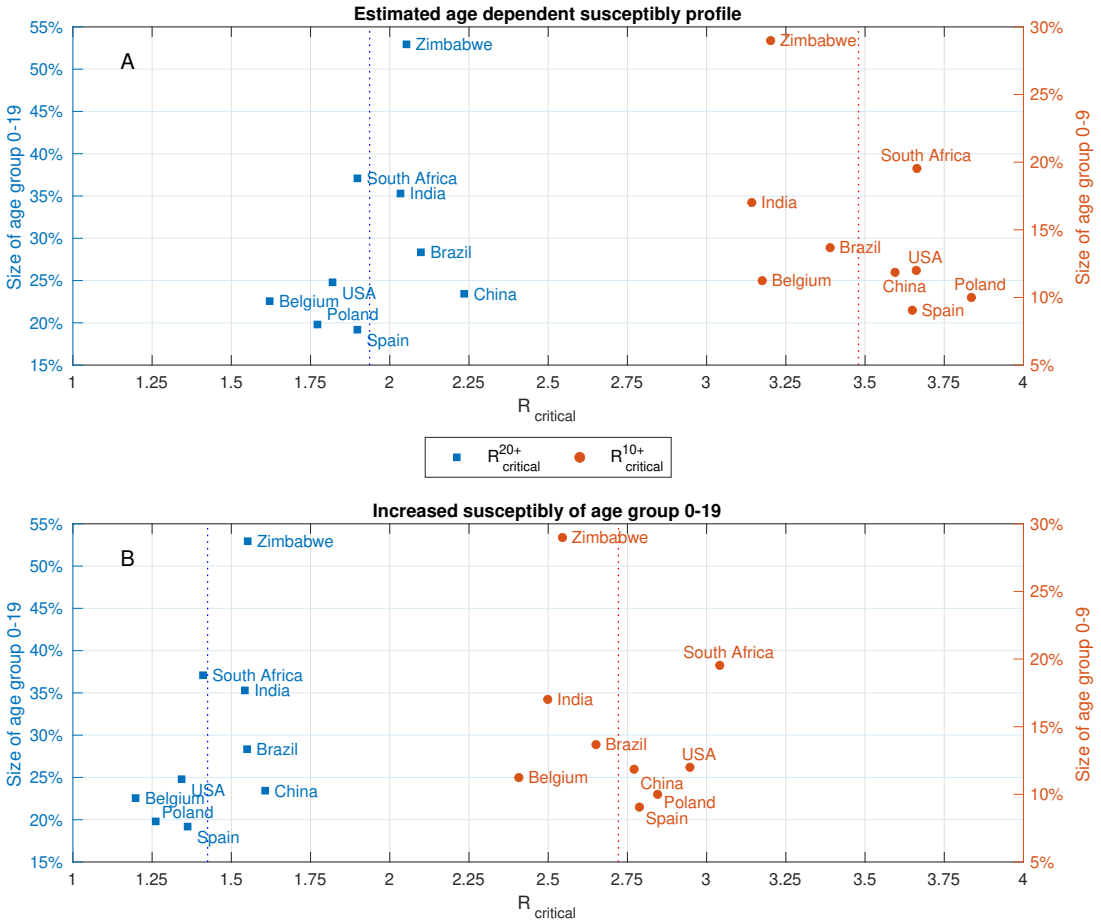

Figure 2: **Critical reproduction numbers.** Reproduction numbers $R^{20+}_{\text{critical}}$ and $R^{10+}_{\text{critical}}$ at which herd immunity cannot be achieved without vaccination of age groups $0-19$ and $0-9$, respectively. Computed using A: age dependent susceptibility profile of SARS-CoV-19 (*4*). B: Same susceptibility profile as in A, but with increased susceptibility of 50% in age group 0-19.

leaky vaccines, see supporting material. We do find, however, that the results are sensitive to changes in the assumptions on relative susceptibility of children.

Sensitivity to the relative susceptibility of children. The examples presented in this study assume the age dependent susceptibility profile of SARS-CoV-19 (*4*) in which the relative susceptibility of age group 0-19 is roughly half of older age groups. Equivalently, one can view age group 0-19 as naturally vaccinated with a leaky vaccine with 50% efficacy in preventing

infections. Accordingly, the results presented in this study show a smaller effect of vaccination of age group 0-19 than in cases in which the relative susceptibility of children is assumed to be higher. In the example presented in Figure 1, we have found that $R^{10+}_{\text{critical}} \approx 3.6$, but if the relative susceptibility of age group 0-19 is increased by 50%, we obtain $R^{10+}_{\text{critical}} \approx 2.9$. Other countries exhibit similar behavior, see Figure 2B. For additional results, see the supplementary material.

Outcomes of a vaccination effort when herd immunity cannot be achieved. We use a final size formula, derived analytically from an age-stratified SIR-type model, which provides the number of individuals per age group that will be infected given a post-COVID basic reproduction number. Expected mortality is then directly computed using an age-dependent infection-fatality ratio. See supplementary materials for code and details.

As an example, we examine the expected outcomes of a vaccination campaign in which 55% of the population of the USA is vaccinated with no age prioritization, i.e., 55% of each age group is vaccinated. Considering a post-COVID basic reproduction number of $R_0 = 3$, we observe that by the end of the epidemic 25.8% of the population above the age of 80 will be infected without the protection of a vaccine, see Figure 3A. When vaccines are homogeneously allocated only to adults (ages 20 and over), the portion of the population above the age of 80 that is infected without the protection of a vaccine drops to 15.7%, but 78.9% of children in the age group of 10-19 are infected, see Figure 3B. The above examples assume that the entire population is either susceptible or vaccinated at the end of the vaccination campaign. In order to model in a more realistic manner we allow for preexisting immunity due to recovery, as well as for the prevalence of active cases, see Figure 3C.

The above results concerning post-vaccination outcomes assumed that vaccine allocation is homogeneous among the eligible age groups. In the following, we consider the extent to which

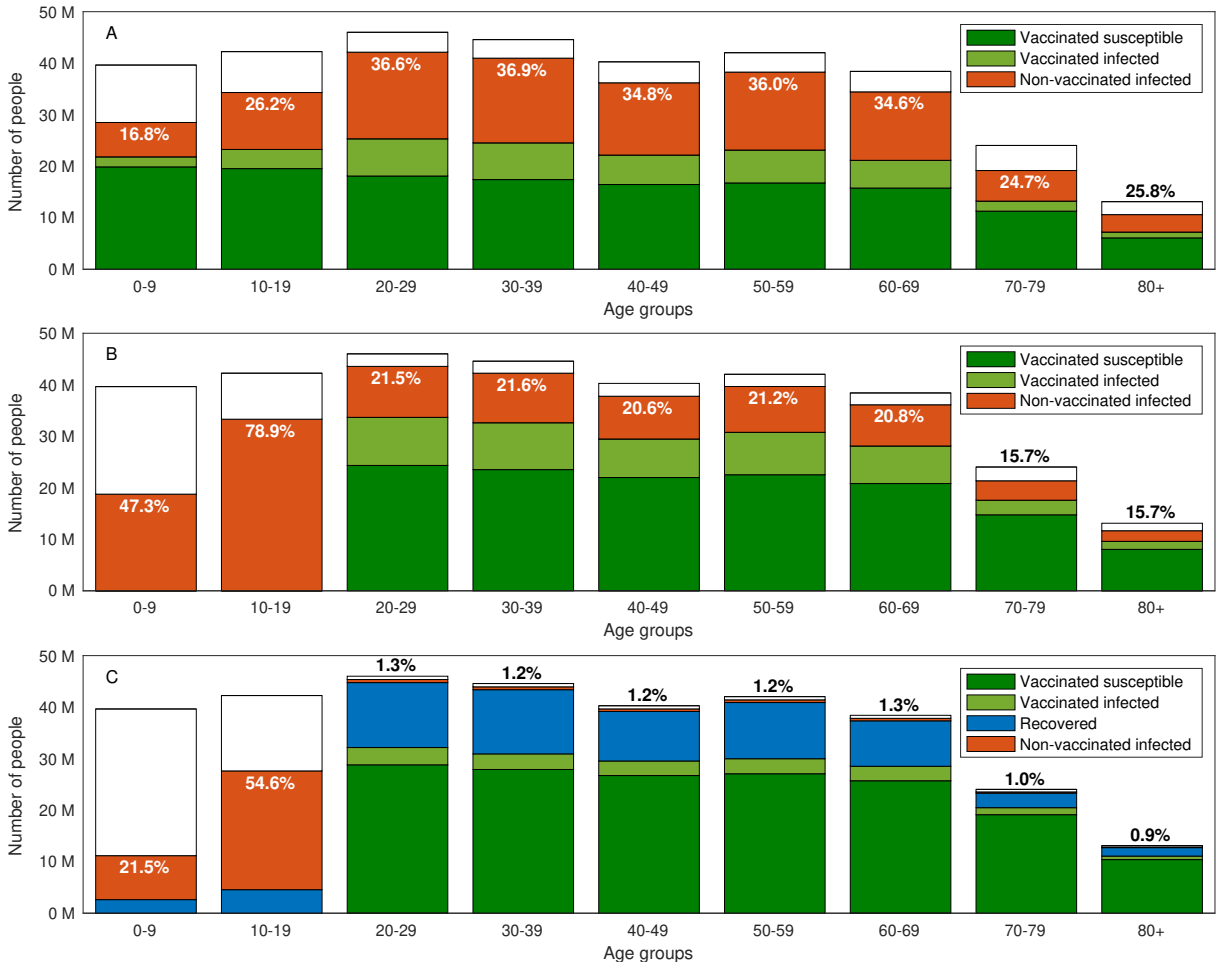

Figure 3: **Final size of epidemic.** The expected outcome of a partial return to normality in the USA to a basic reproduction number of $R_0 = 3$ after completion of a vaccination campaign covering 55% of the population. The computation considers a vaccination campaign in which A: All the population is eligible for vaccinations. B: Vaccine eligibility is limited to ages 20 and above. C: Vaccine eligibility is limited to ages 20 and above, and at the time normality is restored 20% of the population is recovered from COVID-19, and the prevalence of active cases is 0.5% of the population. The text in all graphs corresponds to the percent of non-vaccinated infected individuals in each age group.

an optimized age-dependent allocation can improve the outcomes.

Optimal allocation of vaccines in light of post-vaccination phase outcomes The definition of the term 'optimal outcome', and the corresponding optimal allocation of vaccines, depends on the measure which one aims to optimize. We consider two basic measures which are widely employed: attack rate (overall number of infections), and mortality. It is instructive to plot the possible outcomes in a plane, in which the coordinates of a point correspond to the outcome of a given vaccine allocation in terms of infections and mortality. For example, the yellow points presented in Figure 4A correspond to allocations with a coverage of 55% of the US population, but restricted to adults of age 20 and over (providing coverage of 73.2% of this group), with $R_0 = 3$. The point highlighted with a diamond marker, corresponds to a *pro rata* allocation with no prioritization among those aged 20 and over, giving rise to mortality of half a million individuals and an overall number of 145 million infected individuals. Inspection of random allocations shows that many alternative allocations achieve better outcomes in both senses, namely reduce both infections and mortality, see yellow markers in Figure 4. However, it is not possible to find an allocation that simultaneously achieves optimal outcomes in both senses. Indeed, due to the age-dependent infection fatality ratio there is a trade-off between infections and mortality, e.g., minimizing mortality by vaccination of the elderly results in more infections of the younger age groups. Therefore, we consider the problem as one of multi-objective optimization and generate a curve in the plane of possible outcomes (infections, mortality) which represents the *Pareto front*, the set of outcomes that cannot be improved upon in both senses by changing the allocation, see, e.g., the black solid curve in Figure 4. The choice among outcomes on the Pareto front (and the corresponding vaccine allocations) depends on one's weighing of the importance of the two measures. Application of the Pareto front, which to our knowledge is novel in this context, allows one to systematically evaluate the trade-offs involved among the two measures. The wide range of values along both the infections and the mortality axes shows that these trade-offs are considerable.

The vaccine allocations along the Pareto front are presented in the bottom panel of Figure 4. The left endpoint of the Pareto front represents the outcome corresponding to an allocation chosen so that mortality is minimized, while the right endpoint represents the outcome of the allocation minimizing infections. As expected, the allocation minimizing infections can be seen to prioritize younger age groups, while the allocation minimizing mortality includes older age groups. Moving along the Pareto front we observe a rather complicated structure of variation in the allocations. For example, we see that the 50-59 age group is included in both the allocation minimizing infections and the allocation minimizing mortality, but it is not included in a wide intermediate range along the Pareto front.

We observe that age group 0-9 is not included in the allocations along the Pareto front corresponding to the case in which the entire population is eligible for vaccination. This means that, under the present assumptions, *i.e.*, children are 50% less susceptible than adults, it is sub-optimal to vaccinate children under 10, no matter how the two goals (minimizing infection and mortality) are weighed. On the other hand, age group 10-19 is included in the optimal allocation along nearly the entire Pareto front, except at the right end, corresponding to minimizing of mortality. This implies that restricting vaccination to adults over 20 will worsen outcomes, unless the only outcome of interest is minimization of mortality, in which case those under 20 would not be vaccinated. The extent to which outcomes are worsened by restricting eligibility to those over 20 can be gauged by comparing the two Pareto fronts in the top part of figure 4. Thus, for example, if vaccines are restricted to the 20+ age group, then for $R_0 = 3$ and when an overall of 55% of the population is vaccinated, the minimal number of infections that can be achieved is 114 million, and the allocation achieving this outcome would given rise to a mortality of 1.25 million. If those of age 10-19 become eligible, and an allocation generating the same number of infections is chosen, mortality is reduced by 53% to 0.58 million.

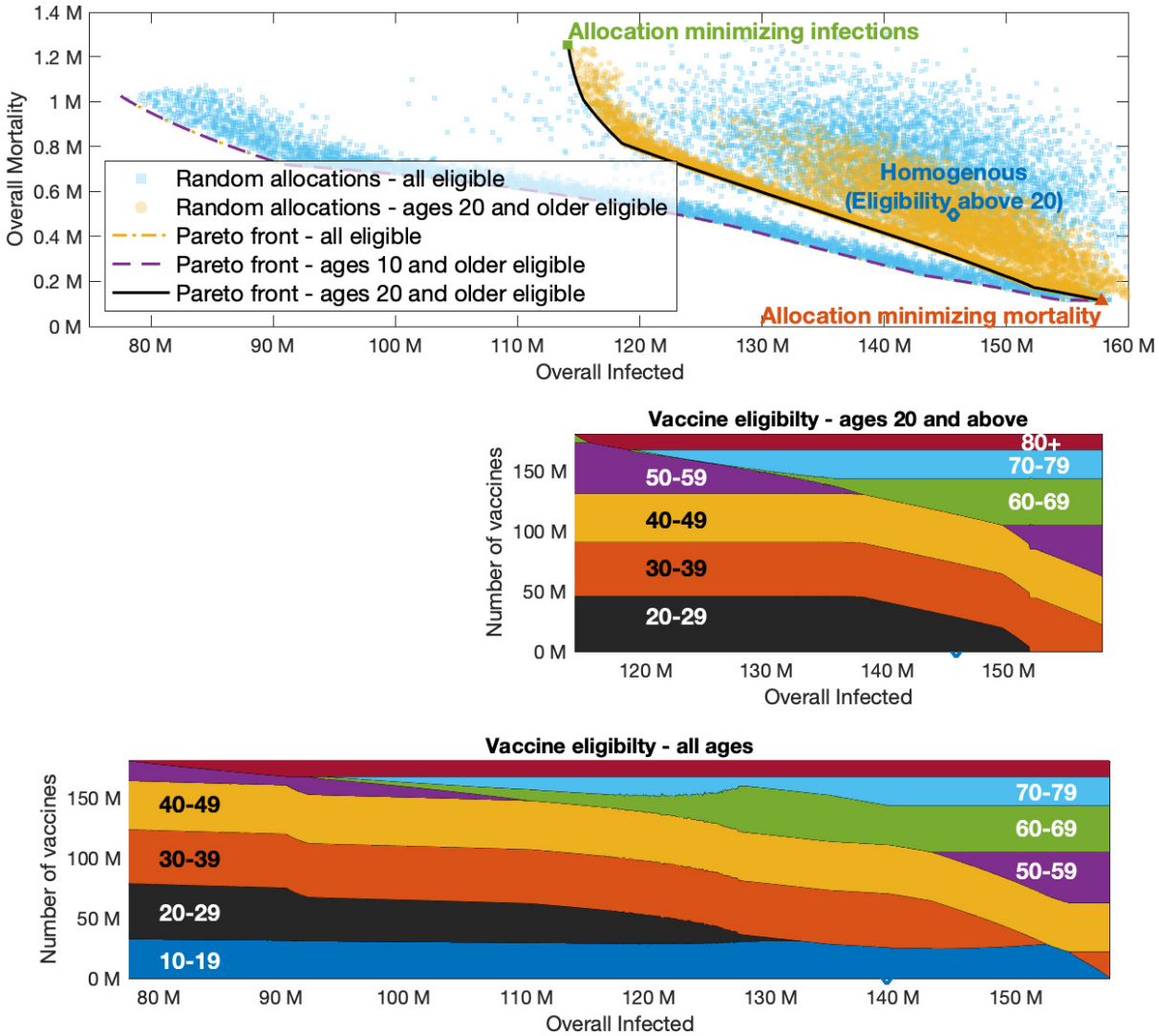

Figure 4: **Pareto front.** Top graph presented outcomes of random allocations when all ages are eligible for vaccination (square blue markers) and only ages 20 and older are eligible (round yellow markers). Super-imposed are the Pareto fronts in the case ages 20 and older are eligible for vaccination (black solid), ages 10 and older are eligible (yellow dash-dotted) and when all ages are eligible (purple dashed). The latter two curves are indistinguishable. Bottom graphs present vaccine allocation along the Pareto fronts in the case of ages 20 and older are eligible for vaccination, and when all ages or ages 10 and older are eligible for vaccination.

Effect of the reproduction number on optimal outcomes There is considerable uncertainty concerning the reproduction number R_0 as it depends on biological features as well as population-specific attributes such as culture, behavior, living conditions etc. Additionally, R_0 may vary in time as result of the emergence of viral variants and the non-pharmaceutical measures in place in the post-vaccination phase. We now examine how the optimal allocations vary with R_0.

Let us first consider the allocation minimizing the number of infections (left part of figure 5). The structure of this allocation, displayed in the bottom panel, varies only slightly with R_0. Particularly, as R_0 increases, the allocation prioritizes younger age groups so that at high values of R_0 a small fraction of this age group 0-9 is vaccinated. In the case of vaccine allocations aimed at minimizing mortality, we observe that for values of R_0 slightly above the herd immunity threshold $R_{\text{threshold}} = R^{10+}_{\text{threshold}} \approx 2.5$, the optimal vaccine allocation for minimizing mortality coincides with the vaccine allocation that ensures herd immunity below the threshold, prioritizing younger ages. In this case, herd immunity is achieved after a rather limited epidemic breakout. At a slightly higher value of R_0, however, a discontinuous shift occurs in the optimal allocation for minimizing mortality. This shift is associated with a large jump in the number of infections. After this shift occurs, the allocation varies only slightly with R_0, except among age groups 10-19 and 30-39. Intuitively, the above cases are characterized by a significant epidemic breakout which leads to high mortality unless vaccines are allocated mostly to those at risk.

Discussion This work demonstrates the use of Pareto front computations to study the outcomes of optimal vaccine allocations, and to systematically evaluate the trade-offs involved among conflicting measures of vaccine allocations such as mortality and attack rate. In particular, we utilize this approach to compare optimal achievable outcomes when all age-groups can be vaccinated to those that can be attained when younger age groups are not eligible for

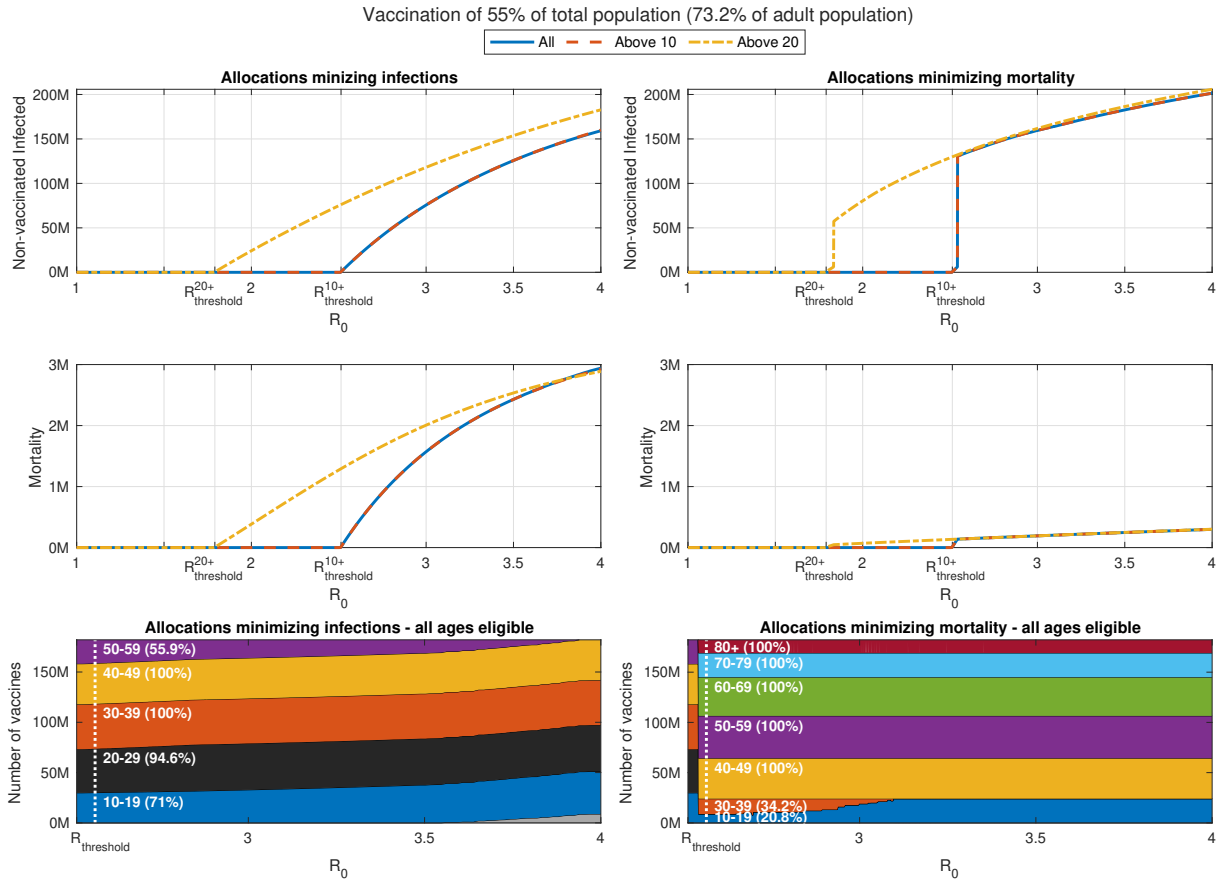

Figure 5: **Impact of change in reproduction number.** Overall infections of non-vaccinated individuals (top graphs) and overall mortality (centered graphs) as function of the basic reproduction number R_0 after completion of a vaccination campaign for allocations minimizing infections (left panels) and allocations minimizing mortality (right panels). The outcomes are presented for the following cases: All ages are eligible for vaccination (solid), only ages 10 and older are eligible (dashes), and only ages 20 and older are eligible (dash-dots). Bottom panels present allocations when all ages are eligible.

vaccination.

Our optimization study points to two main strategies for allocating vaccines when emphasis is given to minimizing mortality, and shows that the optimal strategy sharply transitions between the two as conditions change. The 'herd immunity' strategy aims to reach an effective reproductive number less than one by vaccination, so that the spread of infection is curtailed.

When this strategy is not feasible, the optimization method gives rise to 'protective' allocations that directly protect those populations that are at highest risk of disease complications. The results of this study show that, for a wide range of R_0, a 'herd immunity' strategy is not feasible if vaccination is restricted to ages 20 and older. Indeed, in this case, even if the entire eligible population is vaccinated, the maximal basic reproduction number at which herd immunity can be achieved is around $R^{20+}_{\text{critical}} \approx 2$ and increases only slightly when taking into account existing immunity due to prior infections. When ages 10 and older are eligible for vaccination, optimal allocations can lead to herd immunity for basic reproduction numbers up to $R^{10+}_{\text{critical}} \approx 3.5$, but this threshold varies significantly $(\pm 20\%)$, e.g., among countries and as a result of vaccine coverage and prior immunity. Interestingly, the above thresholds are only weakly correlated with the percentage of children in the population and rather depend on the level of assortativity of mixing within the children sub-population, as reflected in the contact matrix. Although we find that if all age groups, or all ages 10 and above are eligible for vaccination, herd immunity may be achieved at the basic reproduction number of SARS-CoV-19, our results show that the 'herd immunity' strategy is not robust to an increase in R_0, e.g., due to the penetration of more transmissible variants or seasonality. In such a case, mortality would rise steeply since the allocations which aim for herd immunity give preference to the young and leave the older age groups exposed. Thus, even if according to current estimates, the 'herd immunity' strategy (through vaccination) is feasible and is therefore theoretically the optimal strategy, it may not be the strategy of choice given the risks involved in misestimation of parameters or due to a genuine increase in R_0.

When the 'herd immunity' strategy is not feasible and emphasis is given to minimizing mortality, the optimization methods give rise to 'protective' allocations which focus on populations at highest risk of disease complications. Indeed, in all scenarios examined, we observed that vaccines are allocated to the entire population (up to constraints related to hesitancy) in age

groups over 60, and no vaccines are allocated to the age group under 10. In some cases, vaccines were allocated to age group 10-19 but in these cases we observed that the mortality and infections are only marginally reduced relative to allocations which do not include age group 10-19. The 'protective' allocations, however, are associated with a large number of infections. In the example of the USA with 55% and $R_0 = 3$, these allocations result in the infection of roughly 155 million people (45% of the population), mostly from age group 0-19. While the severity of COVID-19 in children is typically very low, such large numbers may carry short or longer-term risks (*2*).

The above two strategies reflect two extremes - prioritization of younger age groups to maximize indirect protection (minimize infections) vs prioritization of older age groups to maximize direct protection (minimize mortality). In this work, we go beyond these two extremes and present a spectrum of Pareto-optimal strategies that give weight to both indirect and direct protection. We show in the USA example that, along the spectrum of strategies, the number of infections varies in the range of roughly 75-155 million people (22-45% of the population). Thus, the trade-off between infections and mortality is substantial. Application of the Pareto front allows one to systematically evaluate these trade-offs. For example, we present a scenario in which a change in the optimal allocation near the mortality minimizing end of the Pareto front (157.5 million infections and 115,000 fatalities) results in a decrease of 5 million infections and an increase of 19,000 fatalities, but a further decrease of 5 million infections results in an additional increase of 49,000 fatalities. Increasing vaccine coverage is an additional way to reduce the number of infections. Our results show that even a slight increase of vaccine coverage may result in a significant reduction in the number of infections. Indeed, we present an example in which an increase from 55% vaccine coverage (as in Figure 4) to 60% vaccine coverage results in a 15% decrease in the number of infections that arise from the optimal allocation at the mortality minimizing end of the Pareto front, and a 50% decrease at the infections minimizing end

(SM I).

When weight is given to both mortality and the number of infections, our results indicate that ineligibility of children of age under 10 will not have a significant effect on the optimal outcomes achievable. However, the ineligibility of the age group 10-19 affects the optimal achievable outcomes in a significant way. In particular, the allocations along the Pareto front considered above all include age group 10-19, and lead to considerably better outcomes compared to the case in which age group 0-19 are not eligible for vaccination as can be observed by the difference between the corresponding Pareto fronts.

We find that the above qualitative picture is robust to changes in the relative susceptibility of children, but the quantitative results are sensitive to the age dependent susceptibility profile of SARS-CoV-19 (*4*) in which the relative susceptibility of age group 0-19 is roughly half of older age groups. Thus, the results presented in this study show a smaller effect of vaccination of age group 0-19 than in cases in which the relative susceptibility of children is higher. This is also true for lower relative infectivity of children (*5*), see also SM N. One implication is that the outcomes of a vaccination campaign and the optimal allocations are sensitive to a misestimation or to changes in the susceptibility and infectivity of children, e.g., due to introduction of lineages to which children are more susceptible.

In this work, we adopt the use of 10-year age groups and accordingly focus on age groups $0-9$ and $10-19$ in the study of the impact of children's vaccination. This allows comparison with other works which use 10-year age groups, e.g., (*6*), or that consider age group $0-19$ as the 'children age-group', e.g., (*9*). This choice of age groups, however, is not in line with the ages for which SARS-Cov-19 vaccination is approved. We consider a sub-division into age groups $12-15$ and $16-19$ in SM M, and show that the qualitative picture is insensitive to this change.

This study is subject to several limitations. We focus on the outcomes in the medium-term

range after the vaccination campaign has ended. Over longer timescales, the possibilities of waning immunity and virus mutation might influence these predictions. Our study optimizes outcomes for the post-vaccination phase, and is, therefore, most relevant when disease spread is contained during the vaccination campaign, e.g., by non-pharmaceutical interventions. In this case, once a vaccine allocation that is optimized for post-vaccination outcomes is determined, transient features of a vaccination campaign that results in the desired allocation can be designed, for example, to allow gradually relaxing non-pharmaceutical interventions during the campaign (*7*). Accordingly, we do not account for increased mortality rates during periods of excessive hospital load (*13*). In case the vaccination campaign occurs in parallel to an ongoing outbreak, short-term goals are likely to dominate the design of the vaccination campaign (*6*). An inherent limitation of any design of a mass vaccination campaign is that not all relevant factors are known in advance, e.g., level of vaccine hesitancy, the overall availability of vaccines, emergence of new lineages, and disease outbreaks. In such circumstances, our work can readily be adapted to optimize the allocation of the remaining available vaccines according to current estimates, taking into account numbers of those already vaccinated, recovered and active infected individuals. Such an approach is demonstrated in the case study of Israel, see SM N.

In this study, we used pre-pandemic contact matrices in accordance with the aim of returning to pre-pandemic routine after the vaccination campaign. Nevertheless, we present results for a range of basic reproduction numbers R_0, and therefore implicitly account for a new routine which includes a degree of non-pharmaceutical interventions. Long-term changes in school operation, however, are not well captured by this approach. Accounting for such age-depended non-pharmaceutical interventions will require the estimation and application of post-pandemic contact matrices.

In the coming months, as vaccine eligibility will be, most likely, expanded to ages 12 and

older and even younger age, we believe that the approach presented in this work can provide model-informed tools to guide the design of vaccine allocations.

References

1. J. Couzin-Frankel, Vaccine trials ramp up in children and adolescents (2021).

2. D. J. Opel, D. S. Diekema, L. F. Ross, *JAMA pediatrics* **175**, 125 (2021).

3. B. L. H. Wong, M. E. Ramsay, S. N. Ladhani, *Archives of Disease in Childhood* (2021).

4. N. G. Davies, *et al.*, *Nature medicine* **26**, 1205 (2020).

5. I. Dattner, *et al.*, *PLoS computational biology* **17**, e1008559 (2021).

6. K. M. Bubar, *et al.*, *Science* **371**, 916 (2021).

7. S. Moore, E. M. Hill, M. J. Tildesley, L. Dyson, M. J. Keeling, *The Lancet Infectious Diseases* (2021).

8. M. T. Meehan, *et al.*, *medRxiv* (2020).

9. L. Matrajt, J. Eaton, T. Leung, E. R. Brown, *Science Advances* **7** (2020).

10. J. Medlock, A. P. Galvani, *Science* **325**, 1705 (2009).

11. F. P. Polack, *et al.*, *New England Journal of Medicine* **383**, 2603 (2020).

12. N. Dagan, *et al.*, *New England Journal of Medicine* (2021).

13. H. Rossman, *et al.*, *Nature Communications* **12**, 1 (2021).

14. M. J. Keeling, P. Rohani, *Modeling infectious diseases in humans and animals* (Princeton university press, 2011).

15. O. Diekmann, J. A. P. Heesterbeek, *Mathematical epidemiology of infectious diseases: model building, analysis and interpretation*, vol. 5 (John Wiley & Sons, 2000).

16. K. Prem, *et al.*, *medRxiv* (2020).

17. *https://population.un.org/wpp* (2019).

18. F. M. Magpantay, M. A. Riolo, M. D. De Celles, A. A. King, P. Rohani, *SIAM Journal on Applied Mathematics* **74**, 1810 (2014).

19. *https://covid19.who.int/* (2021).

Acknowledgments This research was supported by the ISRAEL SCIENCE FOUNDATION (grant No. 3730/20) within the KillCorona – Curbing Coronavirus Research Program.
We are grateful to Dr. Amit Huppert for discussions and valuable comments.

Supplementary material

A SIR model with vaccination

The computations in this work rely on an age-stratified SIR model (*14, 15*). It should be mentioned that since our results concern only the herd-immunity threshold and final sizes, the results derived are identical to those that would be obtained from a more elaborate SEIR or a more general age-of-infection model, since these quantities do not depend on the generation-time distribution (*15*).

The population is divided into n age groups of sizes N_j ($1 \leq j \leq n$). Denote by S_j,I_j,R_j and V_j the number of susceptibles, infected, recovered and vaccinated in group j ($1 \leq j \leq n$). C_{jk} denotes the number of contacts of a single member of age group j with members of group k per unit time. β_j is the probability of infection upon contact for members of group j, allowing for varying susceptibility to infection for different age groups. γ denotes the recovery rate so that $\frac{1}{\gamma}$ is the mean duration of infectivity. $1-\varepsilon$ is the vaccine efficacy against infection - the factor by which probability of infection upon contact is reduced for those vaccinated. In addition we allow for the possibility that for a fraction $1-\nu$ of the population vaccination does not generate immunity. The case $\varepsilon > 0$, $\nu = 1$ is known as 'leaky vaccine', and the case $\varepsilon = 0$, $\nu < 1$ is known as 'all-or-none' vaccine.

We then have the differential equations

$$S_j'(t) = -\beta_j S_j(t) \sum_{k=1}^{n} C_{jk} \cdot \frac{I_k(t)}{N_k}, \tag{1}$$

$$V_j'(t) = -\varepsilon\beta_j V_j(t) \sum_{k=1}^{n} C_{jk} \cdot \frac{I_k(t)}{N_k}, \tag{2}$$

$$I_j'(t) = \beta_j (S_j(t) + \varepsilon V_j(t)) \sum_{k=1}^{n} C_{jk} \cdot \frac{I_k(t)}{N_k} - \gamma I_j, \tag{3}$$

$$R_j'(t) = \gamma I_j(t). \tag{4}$$

We assume that the initial number of infected $I(t_0)$ and of recovered $R_j(t_0)$ are given. A proportion p_j of age group j is vaccinated, so that taking into account that a fraction ν of these will generate immunity, we have

$$V_j(t_0) = \nu p_j N_j, \quad S_j(t_0) = 1 - I_j(t_0) - R_j(t_0) + (1-\nu)p_j N_j.$$

To calculate the basic reproductive number, R_0, we define the next-generation matrix as

$$M = D_\beta C^T D_{\frac{1}{\gamma}},$$

where D_β is a diagonal matrix with diagonal entries β_i, C is the country-specific contact matrix, and $D_{\frac{1}{\gamma}}$ is a diagonal matrix with diagonal entries $\frac{1}{\gamma}$, the infectious period. R_0 is the absolute value of the dominant eigenvalue of M. Similarly, the effective reproduction number R_{eff} is the absolute value of the dominant eigenvalue of

$$M_t = D_\beta D_\sigma C^T D_{\frac{1}{\gamma}}, \tag{5}$$

where D_σ is a diagonal matrix with diagonal entries

$$\sigma_j = 1 - \frac{I_j(t_0) + R_j(0)}{N_j} - (1-\nu)(1-\varepsilon)p_j.$$

B Contact Matrices and Demographics

In all simulations, we used total contact matrices (*16*). Age demographics in all simulations were taken from the UN World Population Prospects 2019 for each country (*17*). Age bins in each case were originally provided in 5-year increment, where the last age bin corresponds to ages 75 and older. We follow the procedure as in (*6*) to adapt the matrices into 10-year increments where the last age bin corresponds to ages 80 and older.

C Computation of vaccine supply threshold

The vaccine supply threshold is the minimal vaccine coverage required for herd immunity. This function is computed via the inverse function. Namely, for each level $0 < p \leq 1$ of vaccine coverage one computes the allocation that assures minimal reproductive number:

$$R_v(p) = \min_{p_1, p_2, \cdots, p_n} \sigma(M_t; p_1, p_2, \cdots, p_n)$$

subject to $0 \leq p_j \leq \frac{S_j(t_0)}{N_j}$ and

$$\sum_{j=1}^{m} p_j N_j = p \sum_{j=1}^{m} N_j,$$

where N_j is the size of age group j, p_j is the portion of age group j that is vaccinated, and $\sigma(M_t)$ is the dominant eigenvalue of the matrix (5). The minimal vaccination coverage required to achieve herd immunity is obtained by solving the equation $R_v(p) = 1$. We conduct these computations using Matlabs' `fmincon` nonlinear programming solver using a sequential quadratic programming algorithm, where the vaccine coverage p is gradually increased and the initial guess used for coverage $p + \delta p$ is adapted from the solution of the optimization problem for vaccine coverage p. The choice of the sequential quadratic programming algorithm is more suitable than the default interior point algorithm used by `fmincon`, since the initial guess provided typically lies on the boundary of the feasible space rather than in its interior.

D Final size formula

The final-size formula yields the overall number of infections taking into account population demography, an age-dependent contact matrix, an age-dependent profile of susceptibility to infection, as well as the percentage of the population in each age group that is vaccinated, recovered, or currently infected, and parameters related to vaccine efficacy in blocking transmission

and preventing disease. To derive it, we reformulate the system (1)-(4) in terms of proportions

$$s_j = \frac{S_j}{N_j}, \quad v_j = \frac{V_j}{N_j}, \quad i_j = \frac{I_j}{N_j}, \quad r_j = \frac{R_j}{N_j}.$$

Obtaining

$$s_j'(t) = -\beta_j s_j(t) \sum_{k=1}^{n} C_{jk} \cdot i_k(t), \tag{6}$$

$$v_j'(t) = -\varepsilon\beta_j v_j(t) \sum_{j=1}^{n} C_{jk} \cdot i_k(t), \tag{7}$$

$$i_j'(t) = \beta_j (S_j(t) + \varepsilon V_j(t)) \sum_{k=1}^{n} C_{jk} \cdot i_k(t) - \gamma i_j(t), \tag{8}$$

$$r_j'(t) = \gamma i_j(t). \tag{9}$$

We assume that the initial number of infected $i(t_0)$ and of recovered $r_j(t_0)$ are given. A proportion p_j of age group j is vaccinated, so that taking into account that a fraction ν of these will generate immunity, we have

$$v_j(t_0) = \nu p_j, \quad s_j(t_0) = 1 - i_j(t_0) - r_j(t_0) + (1-\nu)p_j.$$

From (6),(7) we have

$$\frac{s_j'(t)}{s_j(t)} = -\beta_j \sum_{k=1}^{n} C_{jk} \cdot i_k(t), \qquad \frac{v_j'(t)}{v_j} = -\varepsilon\beta_j \sum_{k=1}^{n} C_{jk} \cdot i_k(t),$$

which upon integration yields

$$\log \frac{s_j(\infty)}{s_j(t_0)} = -\beta_j \sum_{k=1}^{n} C_{jk} \int_{t_0}^{\infty} i_k(s)ds, \quad \log \frac{v_j(\infty)}{v_j(t_0)} = -\varepsilon\beta_j \sum_{k=1}^{n} C_{jk} \int_{t_0}^{\infty} i_k(s)ds,$$

or

$$s_j(\infty) = s_j(0) \exp\left[-\beta_j \sum_{k=1}^{n} C_{jk} \int_{t_0}^{\infty} i_k(s)ds\right], \quad v_j(\infty) = v_j(0) \exp\left[-\varepsilon\beta_j \sum_{k=1}^{n} C_{jk} \int_{t_0}^{\infty} i_k(s)ds\right]. \tag{10}$$

Note that if $s_i(t_0) \neq 0$, then the equations reduce to

$$v_i(\infty) = v_i(t_0) \left(\frac{s_i(\infty)}{s_i(t_0)}\right)^{\varepsilon}.$$

Summing (6)-(8), we have

$$i_j'(t) = -s_j'(t) - v_j'(t) - \gamma i_j(t).$$

Hence,

$$\cancel{i_j(\infty)} - i_j(t_0) = s_j(t_0) - s_j(\infty) + v_j(t_0) - v_j(\infty) - \gamma \int_{t_0}^{\infty} i_j(t),$$

or

$$\int_{t_0}^{\infty} i_j(t) = \frac{1}{\gamma}\left[s_j(t_0) - s_j(\infty) + v_j(t_0) - v_j(\infty) + i_j(t_0)\right]$$

Since $s_j(t) + v_j(t) + i_j(t) + r_j(t) = 1$ for all t, and $i_j(\infty) = 0$, we have

$$s_j(t_0) + v_j(t_0) + i_j(t_0) = 1 - r_j(t_0), \qquad s_j(\infty) + v_j(\infty) = 1 - r_j(\infty), \tag{11}$$

and can write the above as

$$\int_{t_0}^{\infty} i_j(t) = \frac{1}{\gamma}\left[r_j(\infty) - r_j(t_0)\right],$$

so that (10) yields

$$s_j(\infty) = s_j(0)\exp\left[-\frac{\beta_j}{\gamma}\sum_{k=1}^{n} C_{jk}\left[r_k(\infty) - r_k(t_0)\right]\right], \tag{12}$$

$$v_j(\infty) = v_j(0)\exp\left[-\varepsilon\frac{\beta_j}{\gamma}\sum_{k=1}^{n} C_{jk}\left[r_k(\infty) - r_k(t_0)\right]\right]. \tag{13}$$

Combining (11,12,13) yields

$$1-r_j(\infty) = s_j(t_0)\exp\left[-\frac{\beta_j}{\gamma}\sum_{k=1}^{n} C_{jk}\left[r_k(\infty) - r_k(t_0)\right]\right] + v_j(t_0)\exp\left[-\varepsilon\frac{\beta_j}{\gamma}\sum_{k=1}^{n} C_{jk}\left[r_k(\infty) - r_k(t_0)\right]\right],$$

or defining $z_j = r_j(\infty) - r_j(t_0)$ to be fraction of group j infected throughout the post-vaccination period:

$$1 - r_j(t_0) - z_j = s_j(t_0)\exp\left[-\frac{\beta_j}{\gamma}\sum_{k=1}^{n} C_{jk} z_k\right] + v_j(t_0)\exp\left[-\varepsilon\frac{\beta_j}{\gamma}\sum_{k=1}^{n} C_{jk} z_k\right], \quad 1 \le j \le n.$$

Solving this system of equation numerically yields the fractions z_j.

E Computation of an optimal vaccine allocation

For a given vaccine allocation $\{p_i\}_{i=1}^n$ where v_i is the fraction of age group i which is vaccinated, and n is the number of age groups, we use the final size formula to compute the outcomes in terms of the fraction of each age group infected z_j ($1 \leq j \leq n$). The function $f(p_1, p_2, \cdots, p_n)$ to be minimized in the case that the aim is to minimize the number of infections is

$$f_I(p_1, p_2, \cdots, p_n) = \sum_{j=1}^{n} z_j \cdot N_j,$$

while if the aim is minimizing mortality we take

$$f_M(p_1, p_2, \cdots, p_n) = \sum_{j=1}^{n} \eta_j \cdot z_j \cdot N_j,$$

where η_j ($1 \leq j \leq n$) are the fatality rates (IFR) in each age group.

Given the total fraction p of the population to be vaccinated, we consider the following optimization problem (with $f = f_I$, $f = f_M$ or a convex combination of these functions):

$$\min f(p_1, p_2, \cdots, p_n)$$

subject to $0 \leq p_j \leq s_j(0)$ and

$$\sum_{i=1}^{n} p_i N_i = p \sum_{i=1}^{n} N_i \qquad \text{(Total vaccine allocation is equal to vaccine supply)}$$

$$0 \leq v_i \leq s_i \qquad \text{(Vaccine allocation only to known susceptible individuals)}$$

This optimization problem is solved using Matlabs' `fmincon` nonlinear programming solver.

The inequality constraint can be readily modified so that vaccine allocation also does not exceed a given portion α_i of age group i,

$$0 \leq p_i \leq \min(\alpha_i, s_i), \quad i = 1, 2, \cdots, m.$$

This modification enables to account, for example, for vaccine hesitancy, for logistic difficulties in reaching the entire population of an age group, or for a portion of the population who cannot be vaccinated due to medical conditions or allergies.

F Computation of Pareto front

Each point on the Pareto front corresponds to the mortality minimizing vaccine allocation with a given number of infections. To compute the Pareto front, we first compute its endpoints - namely, we compute the infections minimizing vaccine allocation and the mortality minimizing vaccine allocation with corresponding outcomes (I_0, M_0) and (I_L, M_L), respectively, where I is the number of infections and M is the mortality. We conduct these computations using Matlabs' `fmincon` nonlinear programming solver. To avoid convergence of the optimization algorithm to a local minimum, we run the solver with a set of random initial guesses.

The computation of the end points of the Pareto front determines the range of the number of infections along the Pareto front, and allows to determine a grid of L points

$$I_j = I_0 + \frac{I_L - I_0}{L} j, \quad j = 1, \cdots, L,$$

along which the Pareto front is sampled. The optimal allocations along the Pareto front are computed sequentially from one end of the Pareto front to the other by solving the constrained optimization problem of finding the mortality minimizing vaccine allocation with a given number i_j of infections for $j = 1, 2, \cdots, L-1$. The initial guesses used each optimization problem is a set of random allocations around the optimal allocation found for the point $j-1$.

In some cases, we have observed that the direction of sweep from one end to the other is important. To eliminate this factor, we sweep in the opposite direction and if needed update the optimal allocation computed. Namely, we recompute the Pareto front at points I_j for $j = L-1, L-2, \cdots, 1$ where the initial guess for each optimization problem is the optimal allocation found for the point $j+1$.

G Results for all-or-none vaccines

We allow for the possibility that a fraction $1-\nu$ of the population vaccinated does not generate immunity, while the rest of the vaccinated population is fully immune ($\varepsilon = 0$). This case is known as 'all-or-none' vaccine, whereas the case in which all the vaccinated population is partial immune ($0 < \varepsilon < 1$) corresponds to the case of 'leaky' vaccines.

The computation of vaccine supply thresholds and the critical reproduction numbers are indifferent to the 'leaky' or 'all-or-none' nature of vaccine protection. Indeed, these computations rely on the absolute value of the dominant eigenvalue of (5), and thus their dependence on ν and ϵ is only through the expression $(1-\varepsilon)(1-\nu)$.

Leaky vaccines are known to result in a higher prevalence of infection than 'all-or-none' vaccines (*18*). Indeed, for the USA example presented in Figure 4, we observe that allocations along the Pareto front corresponding to 'all-or-none' vaccines give rise to 20% less infections than allocations along the Pareto front corresponding to 'leaky' vaccines, see Figure G. Details of the outcomes of a vaccination campaign with 'all-or-none' vaccines are presented in Figure G. In cases A and B of Figure G, the reductions in overall infections are 28% and 25%, respectively. Finally, we study the impact of vaccine nature on optimal allocation as the reproduction number changes. We observe only a change in the allocation minimizing mortality concerning the allocation of vaccine at the 10-19 or 30-39 age groups.

H Impact of vaccine efficacy

We consider the impact of vaccine efficacy in reducing the susceptibility of those vaccinated on the outcomes of the vaccination campaign.

The relative susceptibility ε of vaccinated individuals effects the vaccine supply thresholds and the critical reproduction numbers solely through the expression $(1-\varepsilon)p_i$ in (5), were p_i is

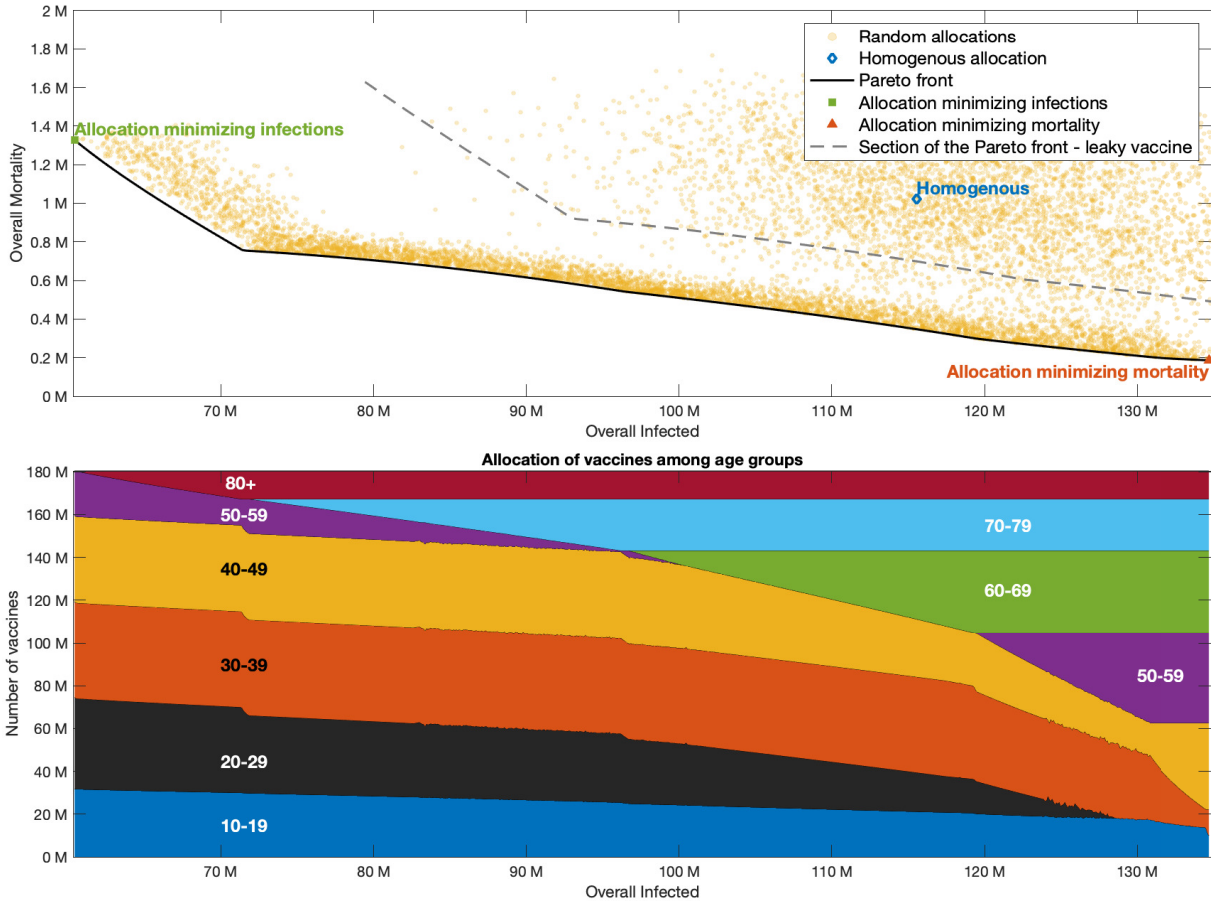

Figure 6: **Pareto front with all-or-none vaccine.** Same as Figure 4, but with 80% all-or-none vaccines. The gray curves in the upper plot correspond to the case of leaky vaccines.

the portion of age group i that is vaccinated. Therefore, in terms of vaccine supply thresholds and the critical reproduction numbers, changes in vaccine efficacy are equivalent to changes in vaccination coverage. As expected, increase of vaccine efficacy lowers the vaccine supply threshold required for herd immunity and vice-versa, see Figure 9. Particularly, children under the age of 10 appear in the allocation that achieves herd immunity with minimal converge at higher values of R_0. Similar behavior is observed in computations adapted for various countries. Particularly, we find that an change of 5% in vaccine efficacy shifted the critical reproduction number $R^{10+}_{\text{critical}}$ by $\Delta R_0 = 0.25$ on average, see Figure 10. However, when only ages 20 and

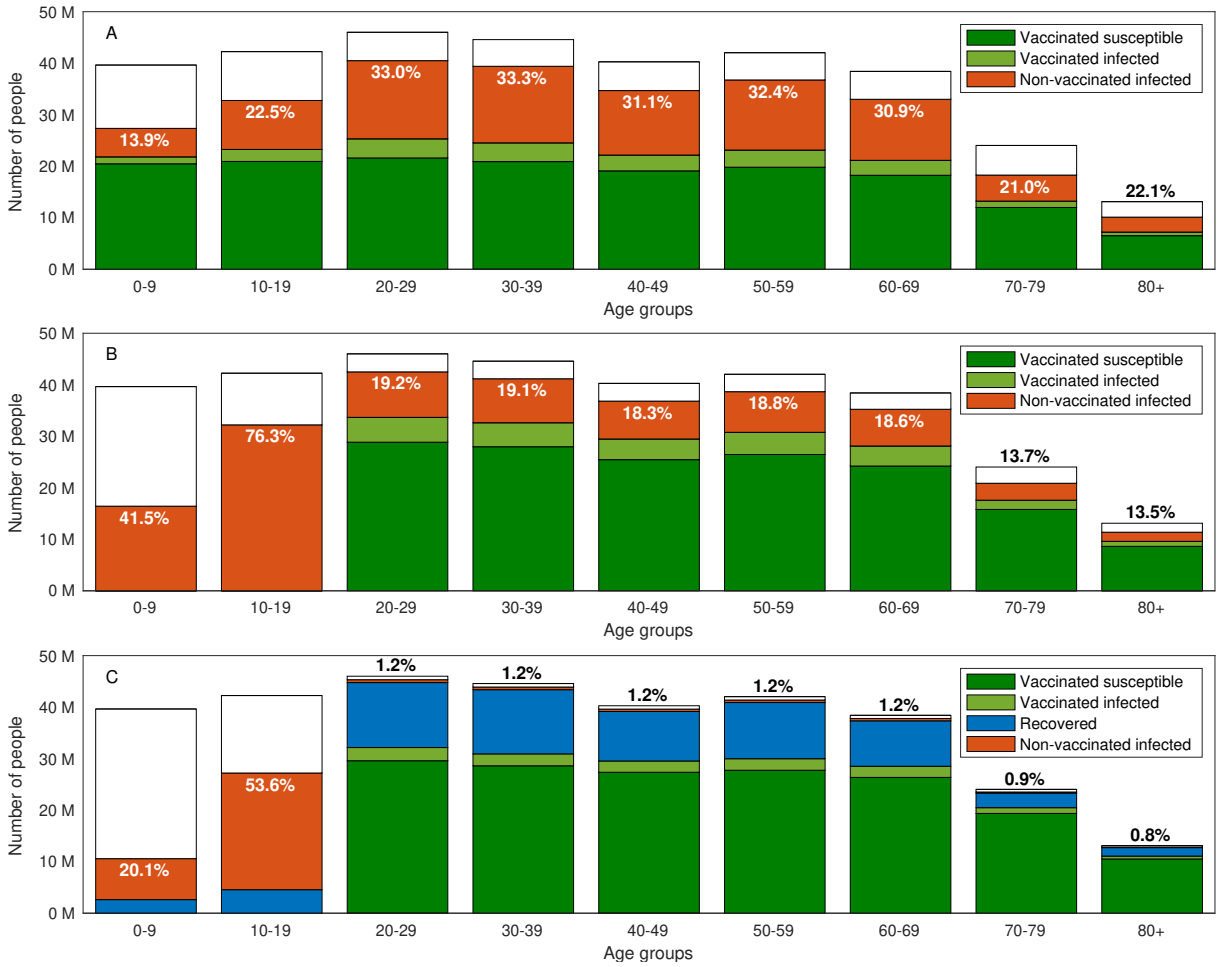

Figure 7: **Final size of epidemic with all-or-none vaccine.** Same as Figure 3 but with all-or-none vaccines: The expected outcome of a partial return to normality in the USA to a basic reproduction number of $R_0 = 3$ after completion of a vaccination campaign covering 55% of the population. The computation considers a vaccination campaign in which A: All the population is eligible for vaccinations. B: Vaccine eligibility is limited to ages 20 and above. C: Vaccine eligibility is limited to ages 20 and above, and at the time normality is restored 20% of the population is recovered from COVID-19, and the prevalence of active cases is 0.5% of the population. The text in all graphs corresponds to the percent of non-vaccinated infected individuals in each age group.

older are eligible for vaccination, the shift in the critical reproduction number $R^{20+}_{\text{critical}}$ is much smaller.

We further consider the impact of vaccine efficacy in cases in which herd immunity is not

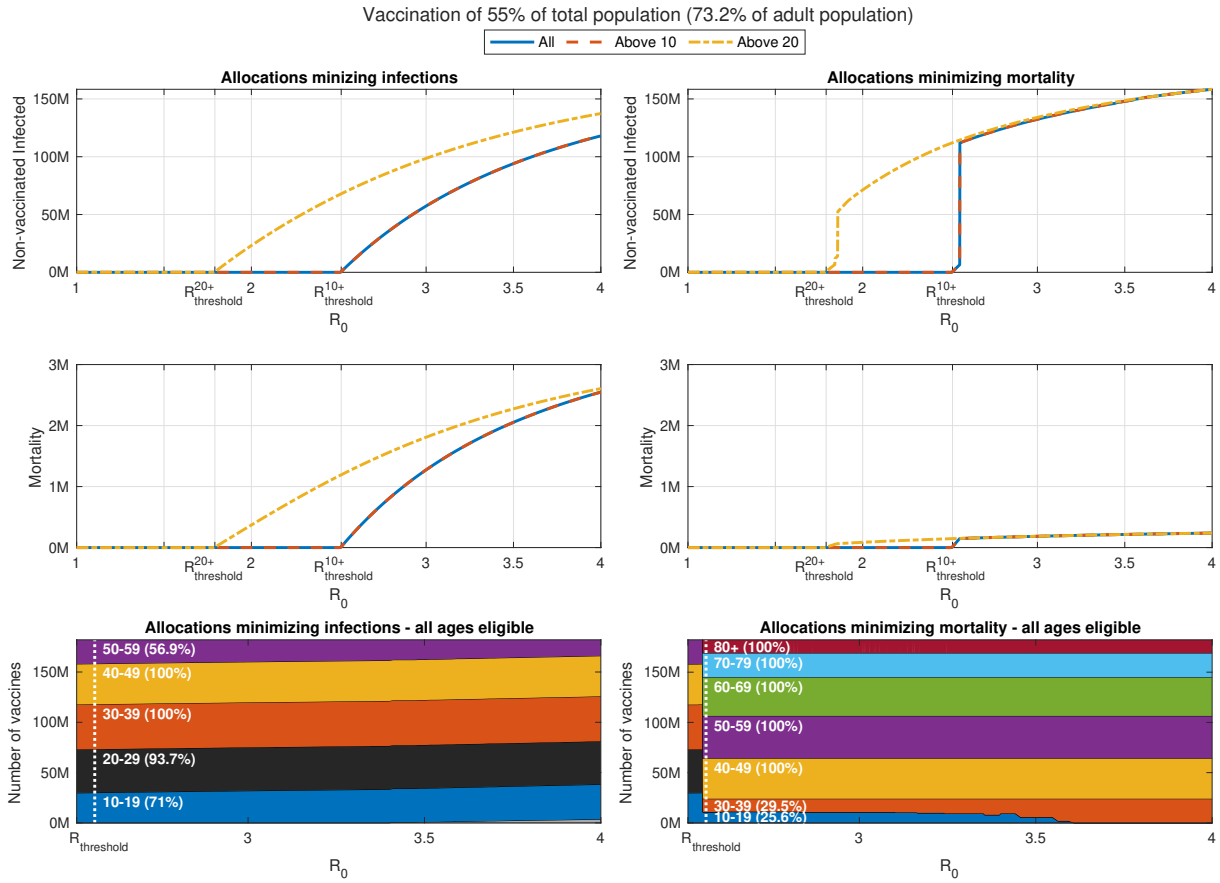

Figure 8: **Impact of change in reproduction number with all-or-none vaccines** Same as Figure 5, but with 80% all-or-none vaccines.

achieved. As expected, the optimal outcomes that result from optimal vaccine distribution along the Pareto front improve with an increase in vaccine efficacy. We observe that a 5% change in vaccine efficacy leads to roughly 33% change in the minimal overall mortality that can be achieved, and 40%-70% change in the minimal overall infections that can achieved by proper vaccine allocation, see Figure H. Moreover, we observe that as vaccine efficacy decreases, the optimal vaccine allocation shifts toward the vaccination of younger ages.

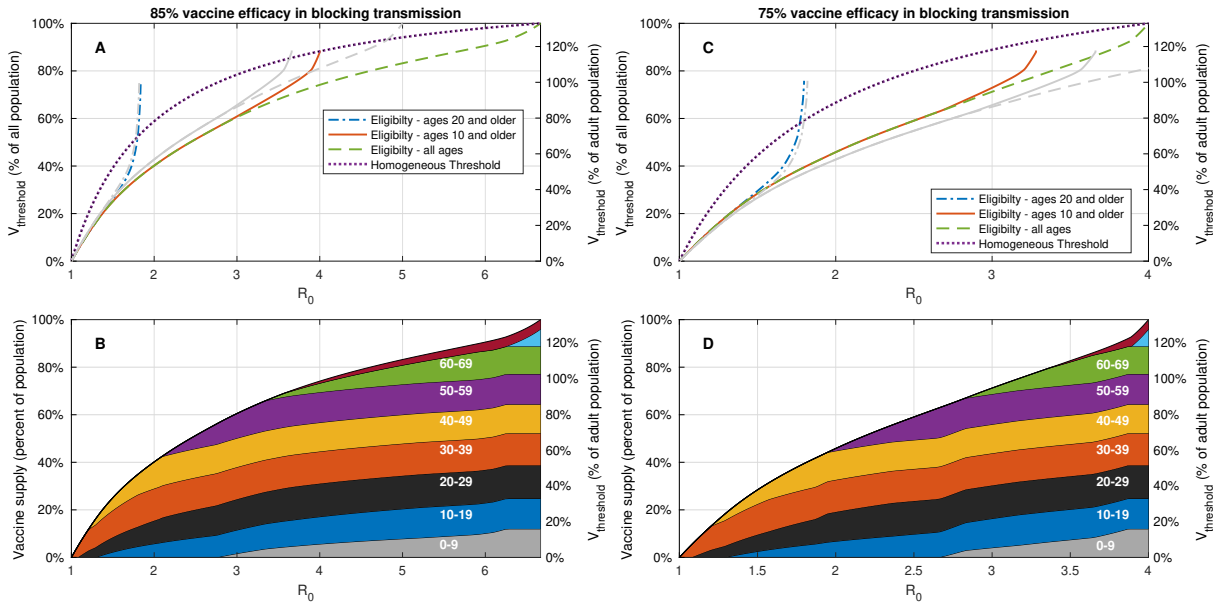

Figure 9: **Effect of vaccine efficacy in blocking transmission (reducing susceptibility) on vaccination coverage required for herd immunity.** A,C: Vaccine coverage $V_{\text{threshold}}$ required to achieve herd immunity threshold as a function of the reproduction number R_0 for the USA demography and contact structure. The gray curves correspond to the case of 80% vaccine efficacy. B,D: Vaccine allocations at which herd immunity is achieved at minimal vaccine coverage and when all the population is eligible for vaccination.

I Impact of vaccine coverage

When herd immunity is not achievable, vaccine coverage becomes a key parameter in the design of a vaccination campaign. As expected, the optimal outcomes that result from optimal vaccine distribution along the Pareto front improve with an increase in vaccine efficacy. We observe that a 5% change in vaccine coverage leads to roughly 20% change in the minimal overall mortality that can be achieved, and 50% change in the minimal number of infections that can achieved by proper allocation of vaccines, see Figure I. The reason for the relatively small change in overall mortality is that already at relatively low vaccine coverage the optimal vaccine allocation for minimizing mortality spans the older age groups, and additional vaccine coverage is mostly utilized to extend allocations to younger age groups which provide indirect protection.

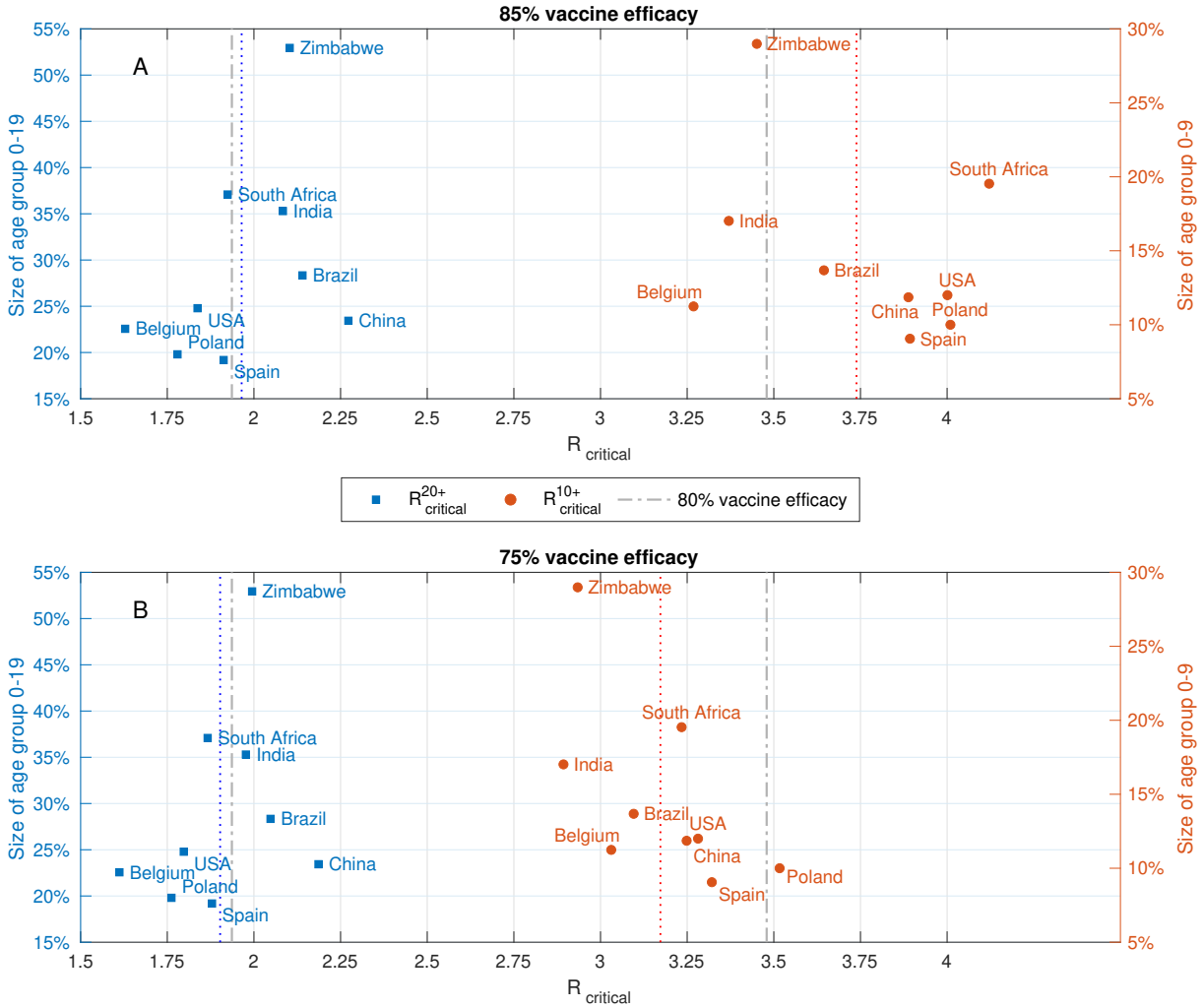

Figure 10: **Effect of vaccine efficacy on critical reproduction numbers.** Reproduction numbers $R^{20+}_{\text{critical}}$ and $R^{10+}_{\text{critical}}$ at which herd immunity cannot be achieved without vaccination of age groups $0-19$ and $0-9$, respectively. Computed for A: 85% vaccine efficacy in blocking transmission. B: 75% vaccine efficacy in blocking transmission. The gray curves in both plots correspond to the case of 80% vaccine efficacy.

J Impact of vaccine hesitancy

The examples presented in Figures 1-5 all consider cases where vaccine allocations can include vaccination of 100% of an age group. However, vaccine hesitancy, logistical difficulties and existing medical conditions are likely to limit actual vaccination coverage within an age group.

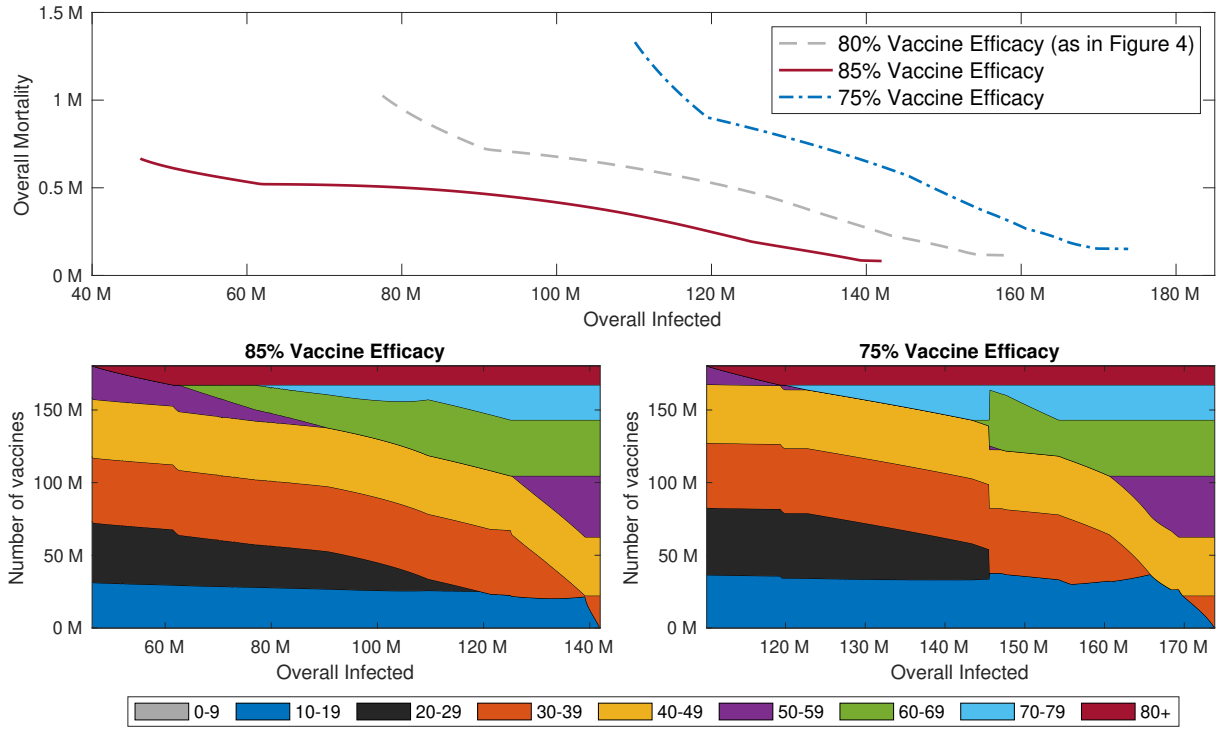

Figure 11: **Pareto fronts for different vaccine efficacy.** Top graphs: Pareto fronts corresponding to 85% (solid red), 80% (dashed gray) and 75% vaccine efficacy (dash-dotted blue). All other parameters are as in Figure 4. Bottom Graphs: Vaccine allocations along the corresponding Pareto fronts with 85% vaccine efficacy (left) and 75% vaccine efficacy (right).

The constraint that vaccine allocation cannot exceed 90% of each age group leads to a significant reduction in the critical reproduction number $R^{10+}_{\text{critical}}$ for which herd immunity is achievable by proper allocation of vaccines from an average of $R^{10+}_{\text{critical}} \approx 3.6$ in various countries to $R^{10+}_{\text{critical}} \approx 3$, see Figure 16. Imposing a stricter constraint that vaccine allocation cannot exceed 80% of each age group, leads to a further reduction to $R^{10+}_{\text{critical}} \approx 2.5$.

We observe that limiting vaccine coverage per age group to 90% results in an 220% increase in the minimal overall mortality that can be achieved and that further limiting vaccine coverage per age group to 80% results in an 330% increase in the minimal overall mortality that can be achieved, see Figure 14. These results strongly suggest that a key performance measure for the

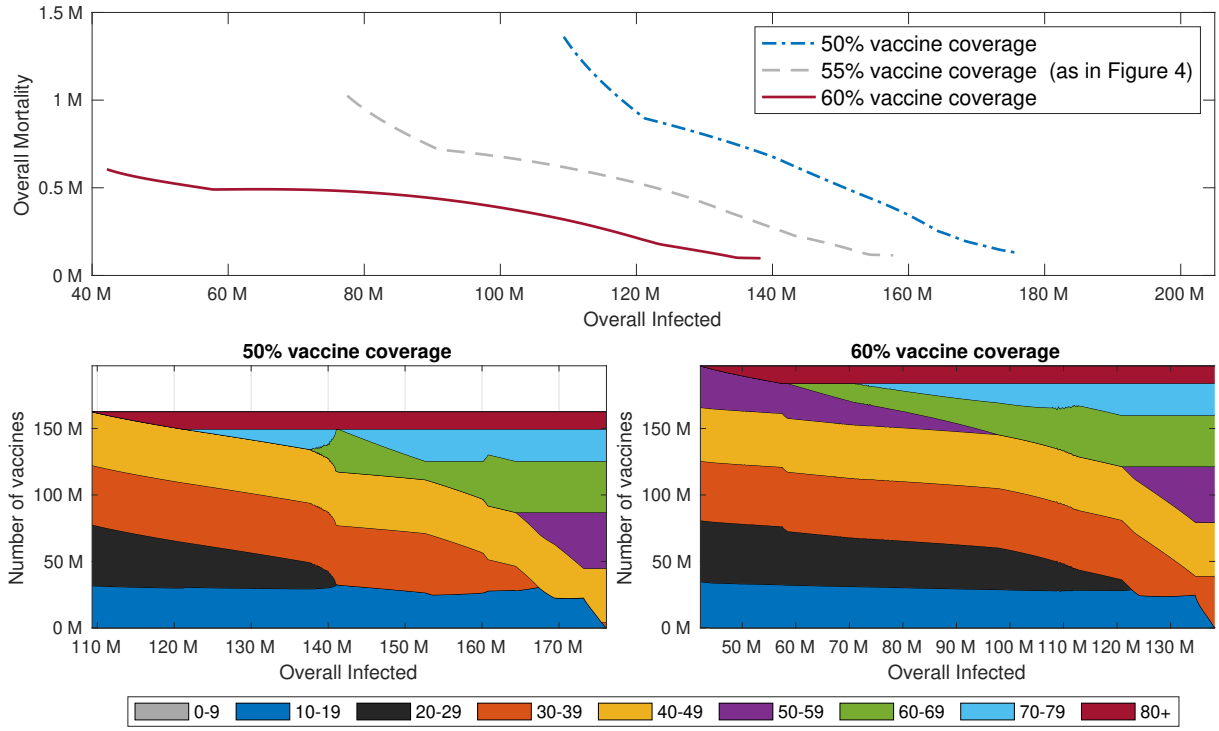

Figure 12: **Pareto fronts for different vaccine coverage.** Top graphs: Pareto fronts corresponding to 50% (solid red), 55% (dashed gray) and 60% vaccine coverage (dash-dotted blue). All other parameters are as in Figure 4. Bottom Graphs: Vaccine allocations along the corresponding Pareto fronts with 50% vaccine coverage (left) and 60% vaccine coverage (right).

success of a vaccination campaign in reducing mortality should be vaccine coverage per age group, particularly in older age groups. In addition, we observe that the minimal number of infections that can achieved by proper allocation of vaccines is not as sensitive to the maximal possible vaccine coverage per age group. Indeed, we find that limiting vaccine coverage per age group to 90% results in 7% increase in the minimal overall mortality that can be achieved and that further limiting vaccine coverage per age group to 80% results in an 19% increase.

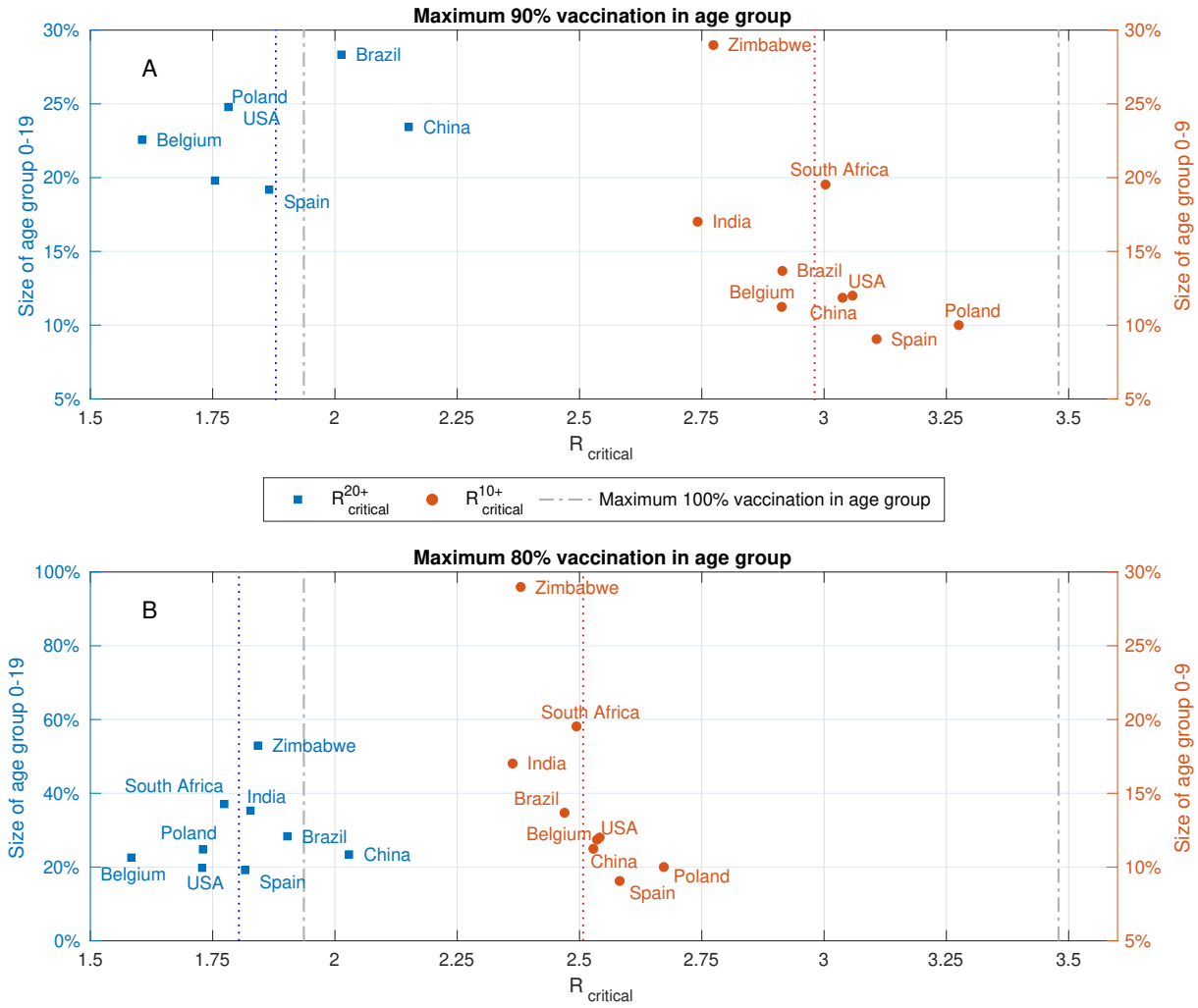

Figure 13: **Effect of vaccine hesitancy on critical reproduction numbers.** Reproduction numbers $R^{20+}_{\text{critical}}$ and $R^{10+}_{\text{critical}}$ at which herd immunity cannot be achieved without vaccination of age groups $0-19$ and $0-9$, respectively. Computed for A: Maximum 90% vaccination in age group. B: Maximum 80% vaccination in age group. The gray curves in both plots correspond to the case when there is no constraint on the number of vaccines that can be allocated to an age group.

K The effect of preexisting immunity in the population due to recovery

Most results presented in this work concerned population which is fully susceptible, unless vaccinated, at the end of the vaccination campaign. In practice, as of April 2021, the number of

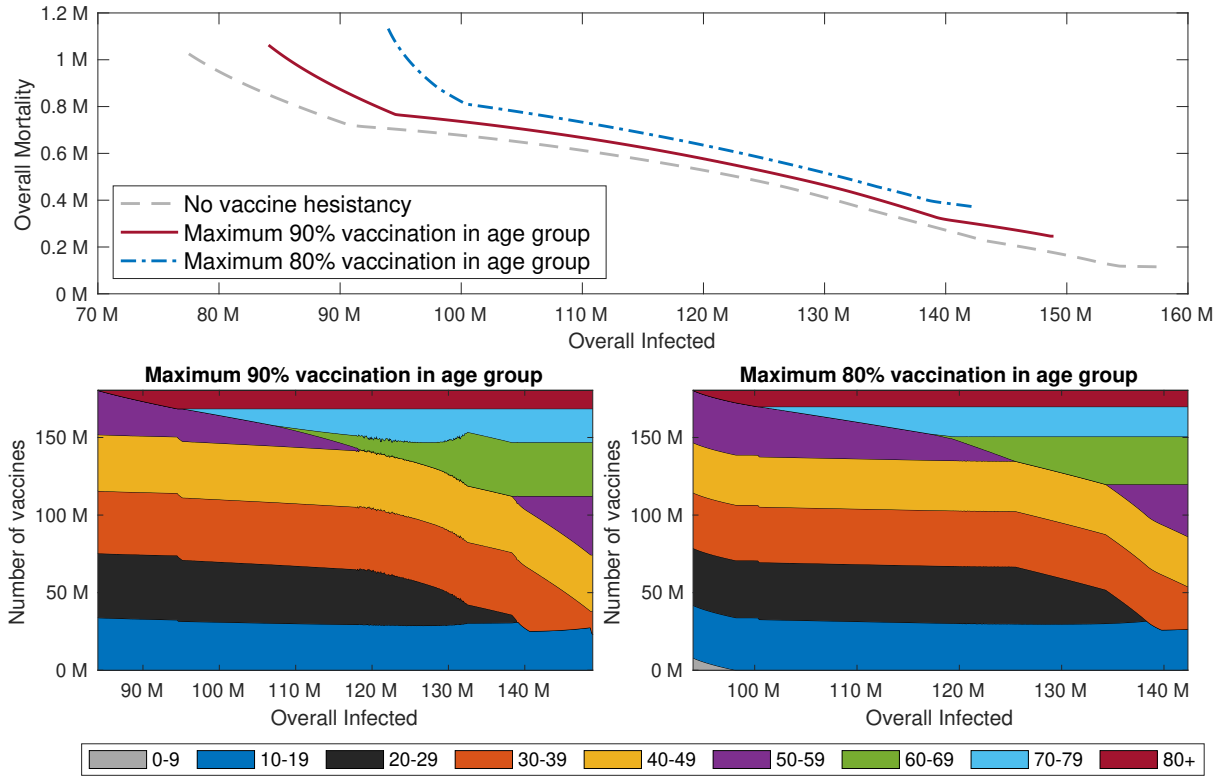

Figure 14: **Pareto fronts for different vaccine hesitancy levels.** Top graphs: Pareto fronts corresponding to a maximum of 90% (solid red), 100% (dashed gray) and 80% vaccine coverage per age group (dash-dotted blue). All other parameters are as in Figure 4. Bottom Graphs: Vaccine allocations along the corresponding Pareto fronts with 90% maximal vaccine coverage per age group (left) and 80% maximal vaccine coverage per age group (right).

COVID-19 cases exceeded 130 million globally (*19*), many of which are recovered. We now study the effect of preexisting immunity in the population due to recovery. In particular, we consider cases in which 10% or 20% of the population are recovered and immune at the end of the vaccination campaign. We determine the distribution of the recovered cases among age groups in a way which is roughly equivalent to running a simulation without any vaccination until the recovered compartments reach the desired size. This is done by determining the distribution of the recovered cases according to the dominant eigenvector of the next generation matrix. A recovered individual is assumed to be fully immune to re-infection. Note, in comparison, that

vaccinated individuals are assumed to be 80% immune to infection. In the computations below, we further assume that vaccines are not allocated to recovered cases.

We first consider the impact of preexisting immunity on vaccination coverage required for herd immunity. As expected, the leading order effect of 10% or 20% preexisting immunity, is that vaccine coverage $V_{\text{threshold}}$ required to achieve herd immunity is reduced by 12% or 25%, respectively, see Figure 15. The differences between the reduction in $V_{\text{threshold}}$ and the percent of population with preexisting immunity stem from the difference in the assumed immunity of recovered and vaccinated, and the fact that preexisting immunity is not optimally distributed.

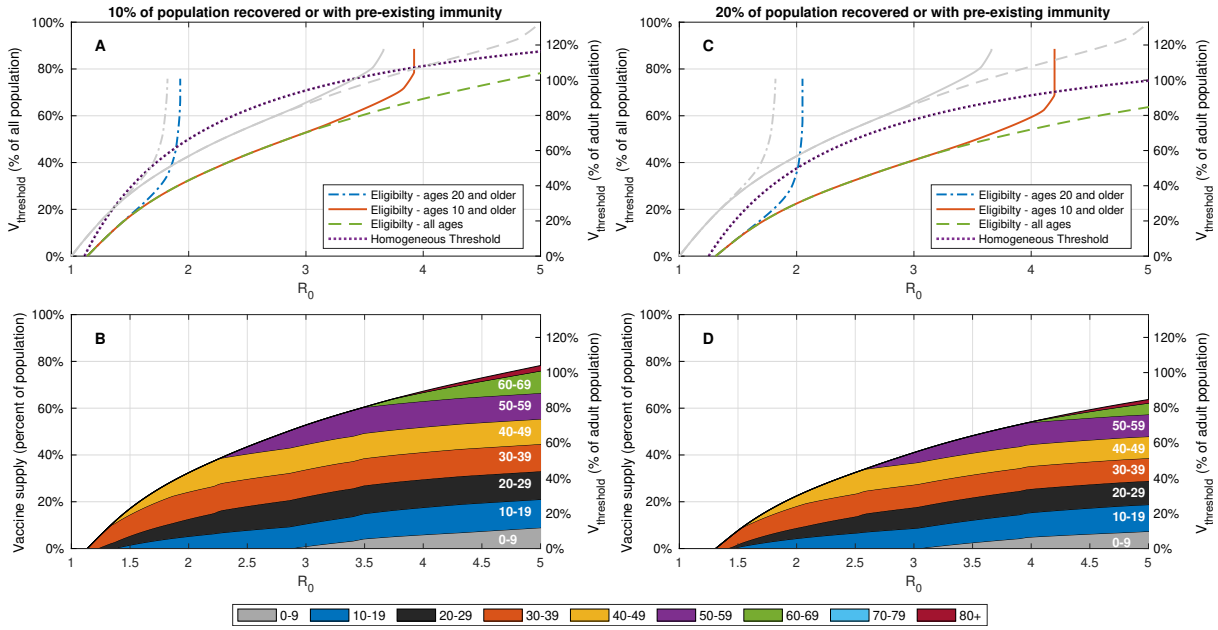

Figure 15: **Impact of preexisting immunity on vaccination coverage required for herd immunity.** A,C: Vaccine coverage $V_{\text{threshold}}$ required to achieve herd immunity threshold as a function of the reproduction number R_0 for the USA demography and contact structure. The gray curves corresponds to the case of no preexisting immunity. B: Vaccine allocations at which herd immunity is achieved at minimal vaccine coverage and when the entire population is eligible for vaccination.

The critical reproduction numbers at which herd immunity cannot be achieved without vaccination of age groups $0-9$ or $0-19$ increase with the percent of the individuals with preexisting

immunity in these age groups. We compute the critical reproduction numbers for nine different countries, and observe that on average, prior immunization of 10% of the population results in the increase of roughly 7% in the critical reproduction numbers $R^{10+}_{\text{critical}}$ and $R^{20+}_{\text{critical}}$. Similarly, prior immunization of 20% of the population results in an increase of about 15% in the critical reproduction numbers $R^{10+}_{\text{critical}}$ and $R^{20+}_{\text{critical}}$.

Next, we compute the Pareto front for the case in which 20% of the population is recovered or has prior immunity and vaccine coverage is 37% of the population (maximal coverage of 50% of population above the age of 20). Vaccines are allocated optimally taking into account the distribution of the recovered population. To study the effect of preexisting immunity, we also consider the case in which none of the population is recovered, but vaccine coverage is 60% of the population. The two scenarios are comparable in the sense that in both of them roughly half the population remains susceptible, where each vaccinated individual is counted as 0.2 susceptible individual to account for 80% vaccine efficacy in blocking transmission. We observe that in the case of preexisting immunity the number of infections along the Pareto front increase by roughly 30% compared to a case of no preexisting immunity, while mortality is only marginally effected, see Figure K. This significant difference stems from the fact that preexisting immunity is not optimally distributed. For example, the optimal allocation for minimizing infections gives rise to an overall number of 42 million infections (left end of dashed gray curve in Figure K), while in the case of preexisting immunity the number of overall infections including the recovered population is bounded below by 66 million people (20% of the population) and reaches 95 million people.

L Impact of age-stratified susceptibility profile

In this work, we have used an age dependent susceptibility profile of SARS-CoV-19 (*4*) in which the susceptibility of individuals in age group 0-19 is roughly half the susceptibility of

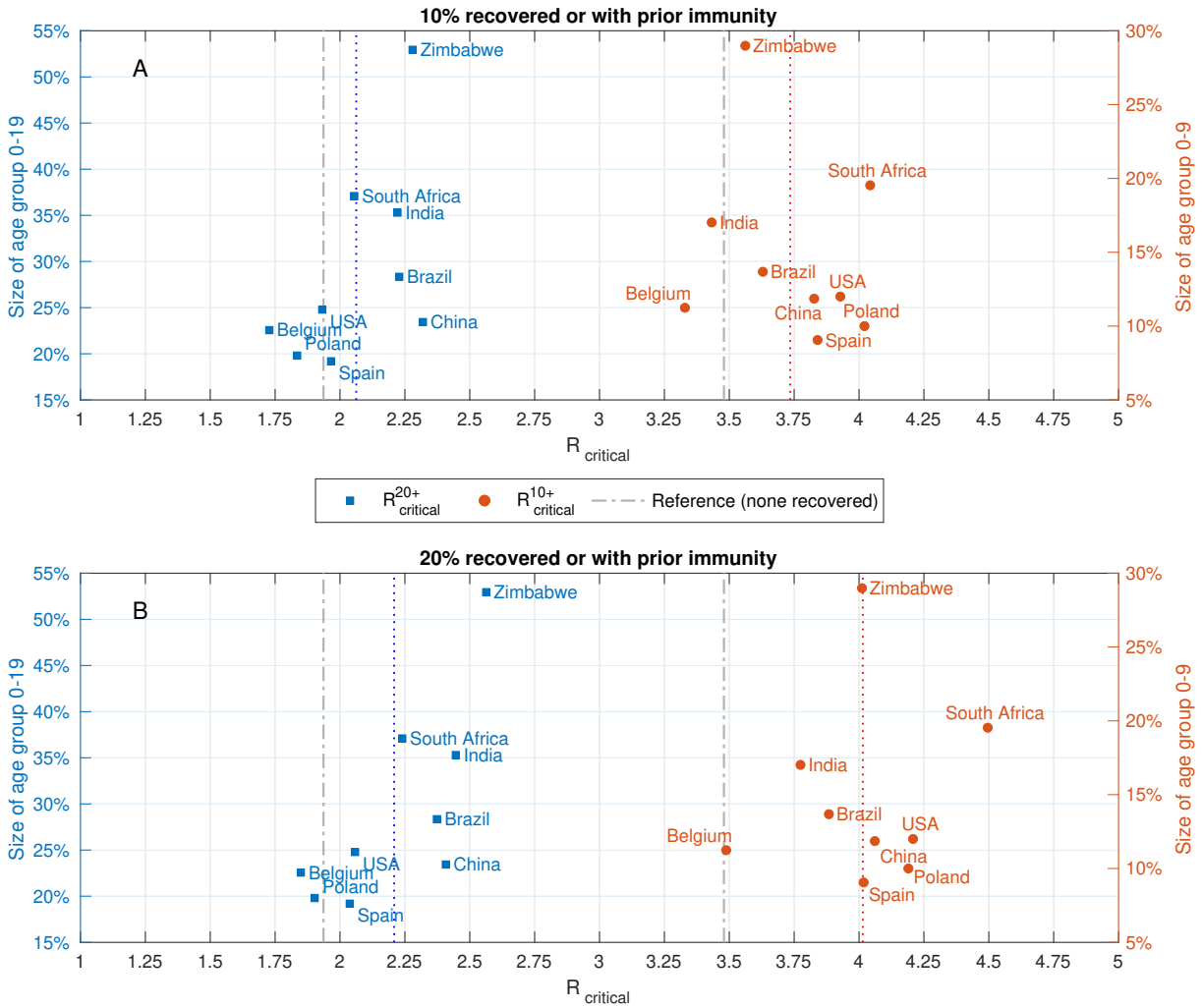

Figure 16: **Impact on preexisting immunity on critical reproduction numbers.** Reproduction numbers $R^{20+}_{\text{critical}}$ and $R^{10+}_{\text{critical}}$ at which herd immunity cannot be achieved without vaccination of age groups $0-19$ and $0-9$, respectively. Computed for A: 10% of the population is recovered or has prior immunity. B: 20% of the population is recovered or has prior immunity. The gray curves in both plots correspond to the case when there is no prior immunity.

those in older age groups. As discussed in the main text, one can equivalently view age group 0-19 as naturally vaccinated with a leaky vaccine with 50% efficacy in preventing infections. Accordingly, the results presented in this study show a smaller effect of vaccination of age group 0-19 than in cases in which the relative susceptibility of children is higher, see, e.g., Figure

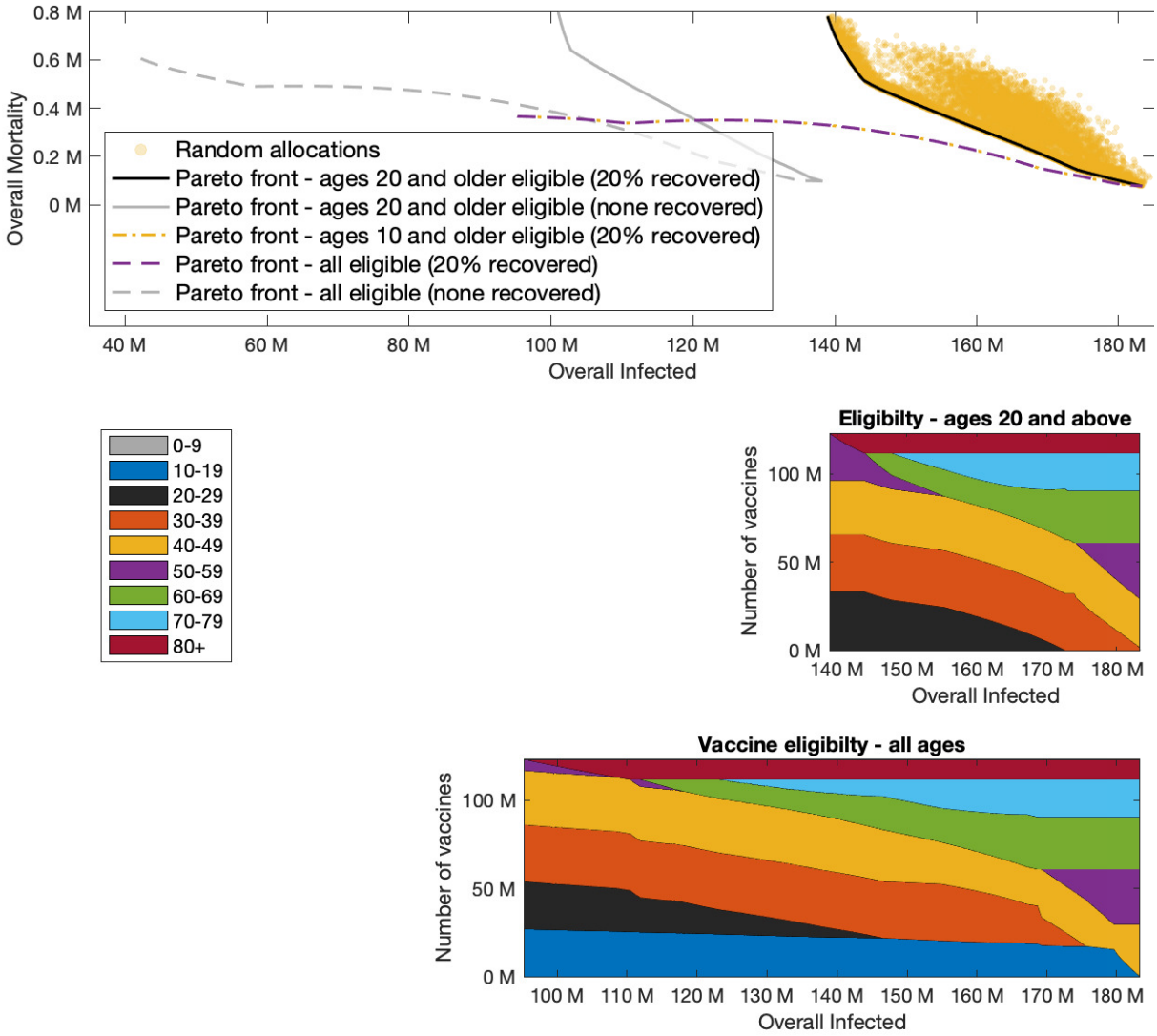

Figure 17: **Pareto front with preexisting immunity.** Pareto fronts computed for the case in which 20% of the population is recovered or has prior immunity and vaccine coverage is 37% of the population. The gray curves in the upper plot correspond to the case of no preexisting immunity and vaccine coverage of 60% of the population. Overall number of infected people includes the number of people recovered or with preexisting immunity.

2B. This can also be observed in Figure 18 presenting the vaccination coverage required for herd immunity and the vaccine allocations that lead to herd immunity at minimal vaccination

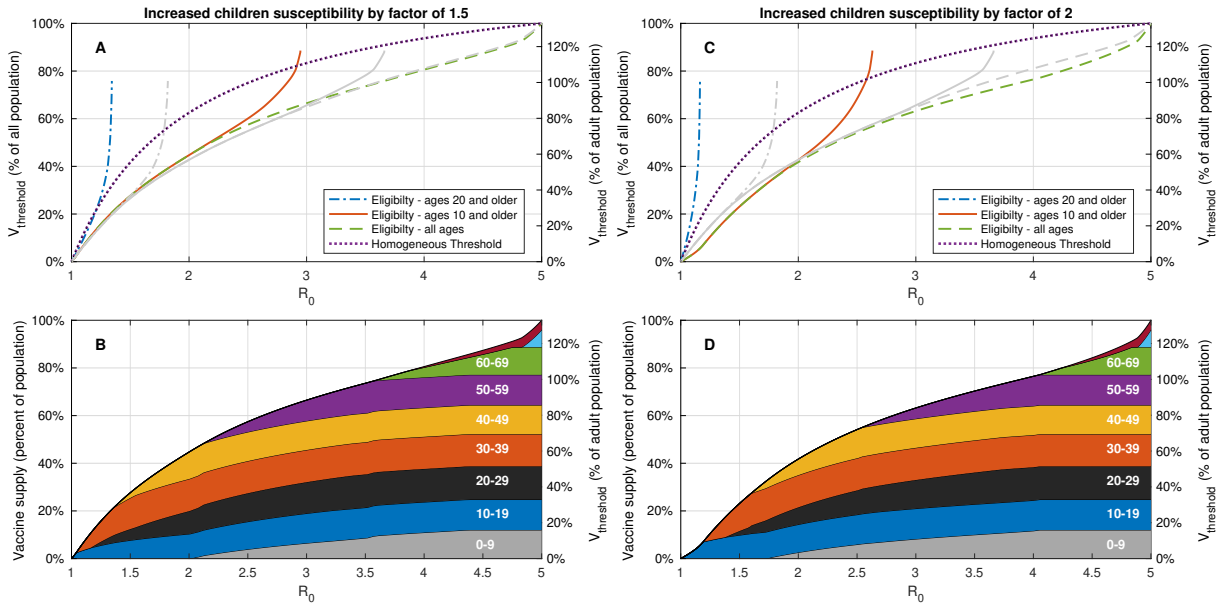

Figure 18: **Effect of change in children susceptibility on vaccination coverage required for herd immunity.** A,C: Vaccine coverage $V_{\text{threshold}}$ required to achieve herd immunity threshold as a function of the reproduction number R_0 for the USA demography and contact structure. The gray curves correspond to the case of 80% vaccine efficacy. B,D: Vaccine allocations at which herd immunity is achieved at minimal vaccine coverage and when all the population is eligible for vaccination.

coverage. As expected, the range of reproduction numbers for which herd immunity can be achieved without vaccination of age group 0-19 narrows from $R_0 < R^{20+}_{\text{critical}} \approx 3.64$ to $R_0 < R^{20+}_{\text{critical}} \approx 2.94$ when the susceptibility of age group 0-19 is increased by a factor of 1.5, and to $R_0 < R^{20+}_{\text{critical}} \approx 2.63$ when the susceptibility of age group 0-19 is increased by a factor of 2 to a level similar to that of older age groups.

We note that unlike the other parameters considered in this work, the change in the susceptibility profile changes the epidemic spread in the absence vaccines. In particular, the definition of the basic reproduction number depends on the susceptibility profile. Therefore, it is meaningless to compare the effect of changing different susceptibility profiles by considering epidemic outcomes at the same basic reproduction number. For this reason, we do not present graphs

of Pareto fronts for different susceptibility profiles at a given reproduction number. Rather, we present graph that show how vaccine allocation changes over a range of reproduction numbers for different susceptibility profiles. As expected, as the susceptibility of children is higher, the allocations minimizing infections dedicate larger portions of vaccines in age group 0-19, see Figures 19 and 20. Nevertheless, the allocations minimizing mortality do not change.

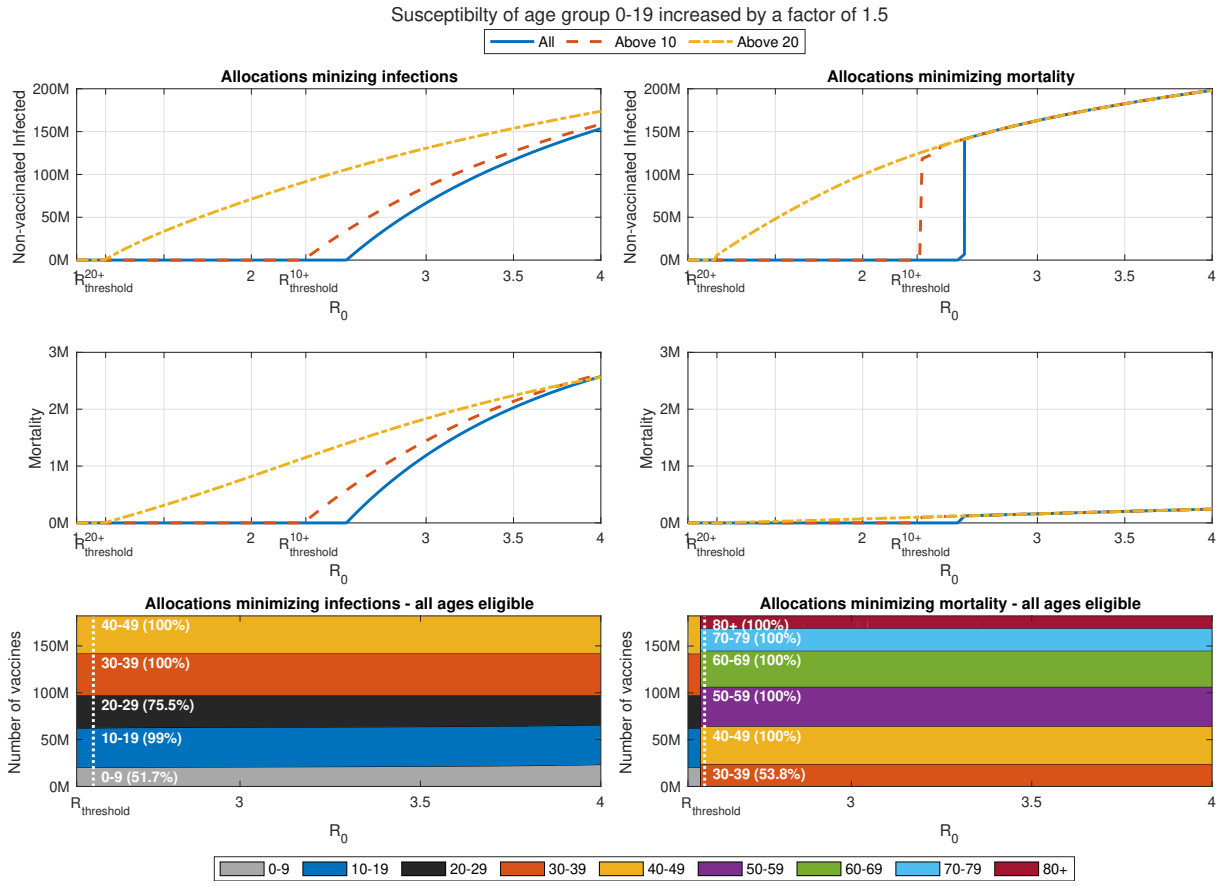

Figure 19: **Impact of change in reproduction number when susceptibility of age group 0-19 is increased by factor of 1.5.** Same as Figure 5 except the susceptibility of age group 0-19 is increased by factor of 1.5.

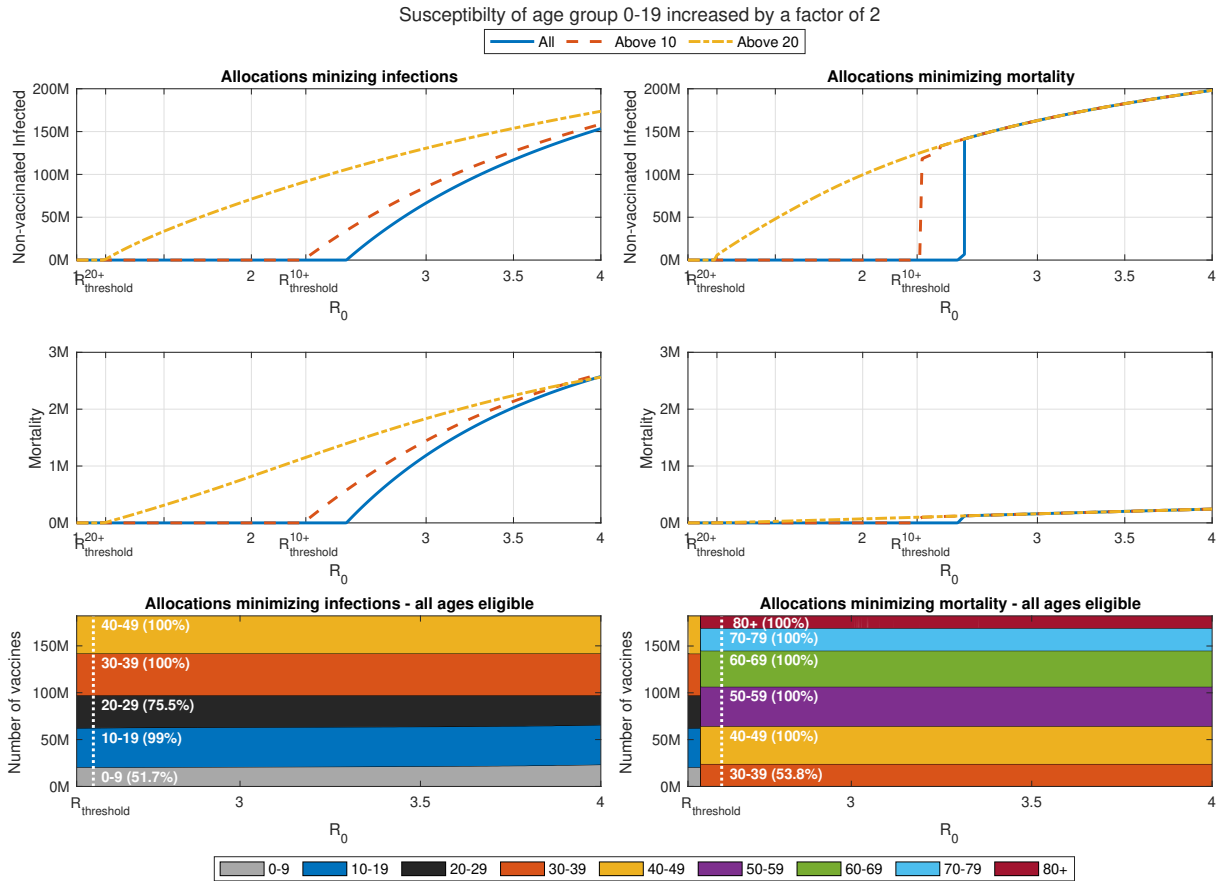

Figure 20: **Impact of change in reproduction number when susceptibility of age group 0-19 is increases by factor of 2.** Same as Figure 5 except the susceptibility of age group 0-19 is increases by factor of 2.

M Age groups $12-15$ and $16-19$

In this work, we adopt the use of 10-year age groups and accordingly focus on age groups $0-9$ and $10-19$ in the study of the impact of children's vaccination. This allows comparison with works which use 10-year age groups, e.g., (*6*), or that consider age group $0-19$ as the 'children age-group', e.g., (*9*). This choice of age groups, however, is not in line with the ages for which SARS-Cov-19 vaccination is approved. Indeed, currently ages 16 and older are eligible for SARS-Cov-19 vaccines, and efforts are focused on extending vaccine approval for children

above 12 (*1*). Here, we consider the cases in which only individuals of ages 12 and older, or those of ages 16 and older, are eligible for vaccination. To do so, we assume that the contact structure and relative susceptibility is uniform within the 10-19 age group, and model limited eligibility within age group 10-19 by restricting the number of vaccines that can be allocated to this age group. Particularly, we restrict number of vaccines that can be allocated to age group 10-19 to 80% of the age group in the case of ages 12 and older, and 40% in the case of ages 16 and older.

As expected, the critical reproduction number $R^{12+}_{\text{critical}}$, for which reaching herd immunity becomes impossible if children under the age of 12 are not vaccinated, is slightly shy of $R^{10+}_{\text{critical}}$. Similarly, $R^{16+}_{\text{critical}} \approx 2.53$, in close agreement with the interpolated value between $R^{20+}_{\text{critical}} \approx 1.81$ and $R^{10+}_{\text{critical}} \approx 3.64$. We further extend the example of Figure 4 and consider the Pareto fronts when vaccine eligibility is restricted to ages 12 and older, or ages 16 and older. We observe that the Pareto front corresponding to vaccine eligibility for ages 12 and older is indistinguishable from the Pareto front corresponding to the case when all ages are eligible for vaccination. The reason is that, in the scenario examined in Figure 4, the vaccine allocations along the Pareto front corresponding to the case when all ages are eligible for vaccination, reach a maximum of 77% vaccine allocation to age group 10-19. Therefore, the restriction to ages 12 and older, which is modelled by a constraint of maximum 80% allocation to age group 10-19, does not impact the allocation along the Pareto front. However, imposing a constraint of maximum 40% allocation to age group 10-19 to model vaccine eligibility to ages 16 and older, does impact the allocation along the corresponding Pareto front. Indeed, The allocations along the Pareto front corresponding to the case in which vaccine eligibility is restricted to ages 16 and older give rise to higher numbers of overall infections, but do not impact the mortality-minimizing end.

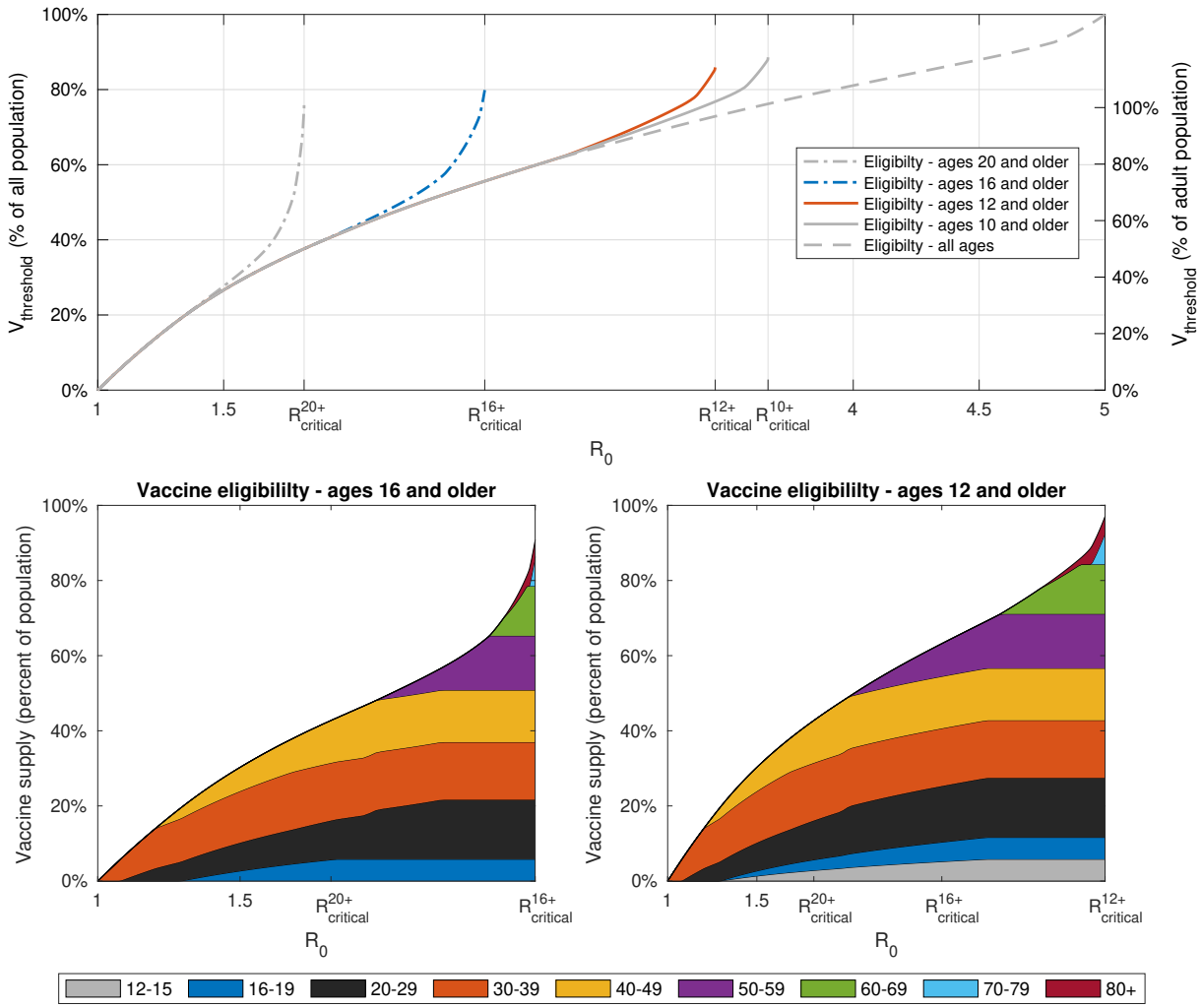

Figure 21: **Vaccination coverage required for herd immunity - age groups 12-15 and 16-19.** Top graph: Vaccine coverage $V_{\text{threshold}}$ required to achieve herd immunity threshold as a function of the reproduction number R_0 for the USA demography and contact structure. The gray curves corresponds to the case of vaccine eligibility in age groups 20+, 10+ and all ages. Bottom graphs: Vaccine allocations at which herd immunity is achieved at minimal vaccine coverage and when ages 16 and above, and ages 12 and above, are eligible for vaccination.

N Real-data: Israel as a case study.

We supplement this work by applying the tools developed in this study to a case study with real-data. In the following, we consider Israel. Relevant data, updated to Mid April 2021, is acquired

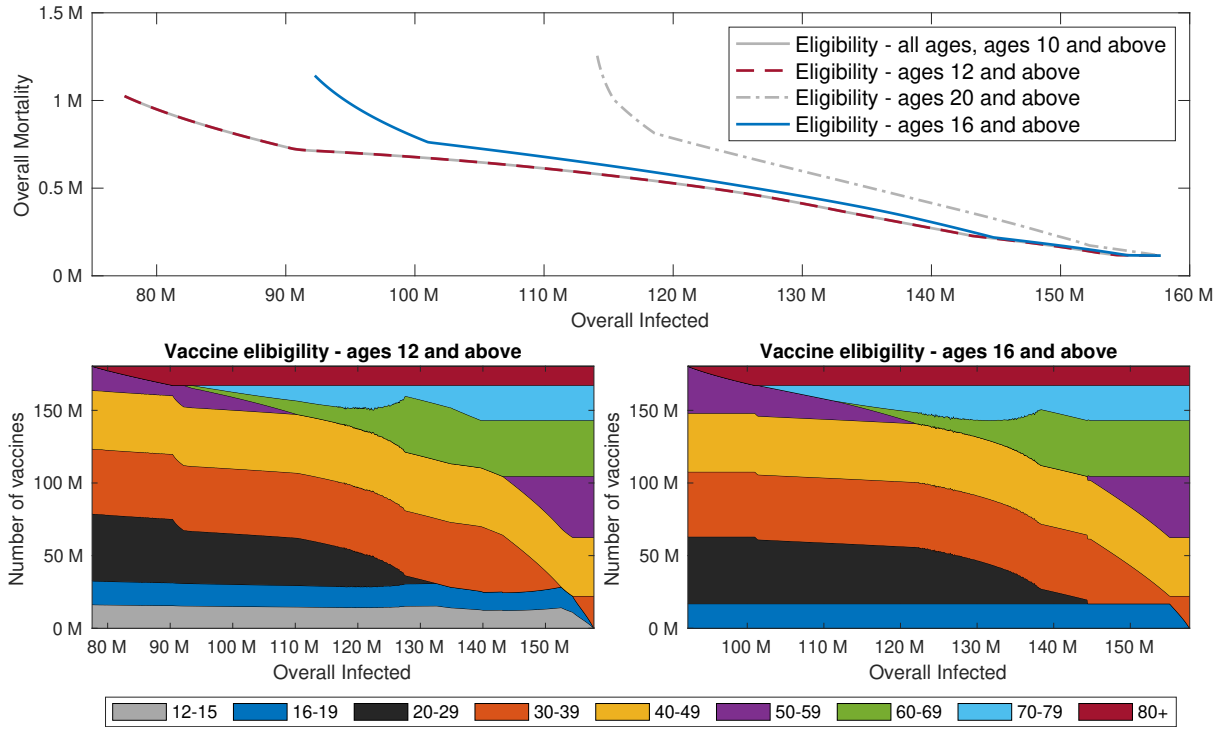

Figure 22: **Pareto fronts with age groups 12-15 and 16-19.** Top graphs: Pareto fronts corresponding to vaccine eligibility for: all ages or ages 10 and older (solid gray curve), ages 12 and older (dashed red), ages 16 and older (solid blue) and ages 20 and older (dash-dotted gray). All other parameters are as in Figure 4. The curves for all ages, ages 10 and older, and ages 12 and older are indistinguishable. Bottom Graphs: Vaccine allocations along the corresponding Pareto fronts when vaccine eligibility is for ages 12 and older (left), and ages 16 and older 50% vaccine efficacy (right).

from the Israeli ministry of health, and parameters such as contact matrices, detection rates, age-dependent mortality rates and more are customized to Israel. An account of the statistical analysis and calibration procedures used to extract these parameters will be presented elsewhere. We note that the data and parameters presented in the section are in compliance with the data organization and with other models used by the ministry of health of Israel. In particular, they do not fully agree with the parameters presented in this work as those were chosen in compliance to other works to allow comparisons. A key difference is that we assume that the relative susceptibility of age group 15-19 is the same as adults, while the relative susceptibility of age group 0-14 is the half of older age groups (as in this work). We further assume that the infectivity of age group 0-14 is 3/4 that of older age groups (*5*). We use 5-year age groups which enables capturing this heterogeneity in age group 10-19.

As of mid April, 55% of the Israeli population has been vaccinated with at least one vaccine shot. Vaccination policy first emphasized vaccination of the population of age 60 and older, but eventually vaccines were made available to all the eligible population, namely ages 16 and older. This policy resulted in the vaccination of roughly 90% of the population above the age of 50, 76% of the population in age group 20-49 and 50% of the population in age group 16-19. Additionally 8.4% of the population is known to be recovered, and we further estimate that an additional 10.7% of the population had recovered from SARS-CoV-19 but were never detected. The latter estimate is also used to approximate the number of vaccines administered to individuals who were already recovered.

Using the final size formula, we estimate that Israel has achieved herd immunity for up $R_0 \approx 2.6$. As of mid-April, the basic reproduction number is estimated to be lower than $R_0 = 2$, and NPIs include wearing of masks in public spaces, partial operation of the school system, and restriction of indoor activities, e.g., in restaurants or in concerts, as well as of large gatherings to those vaccinated or recovered. At the time of submission, wearing of masks outdoors be-

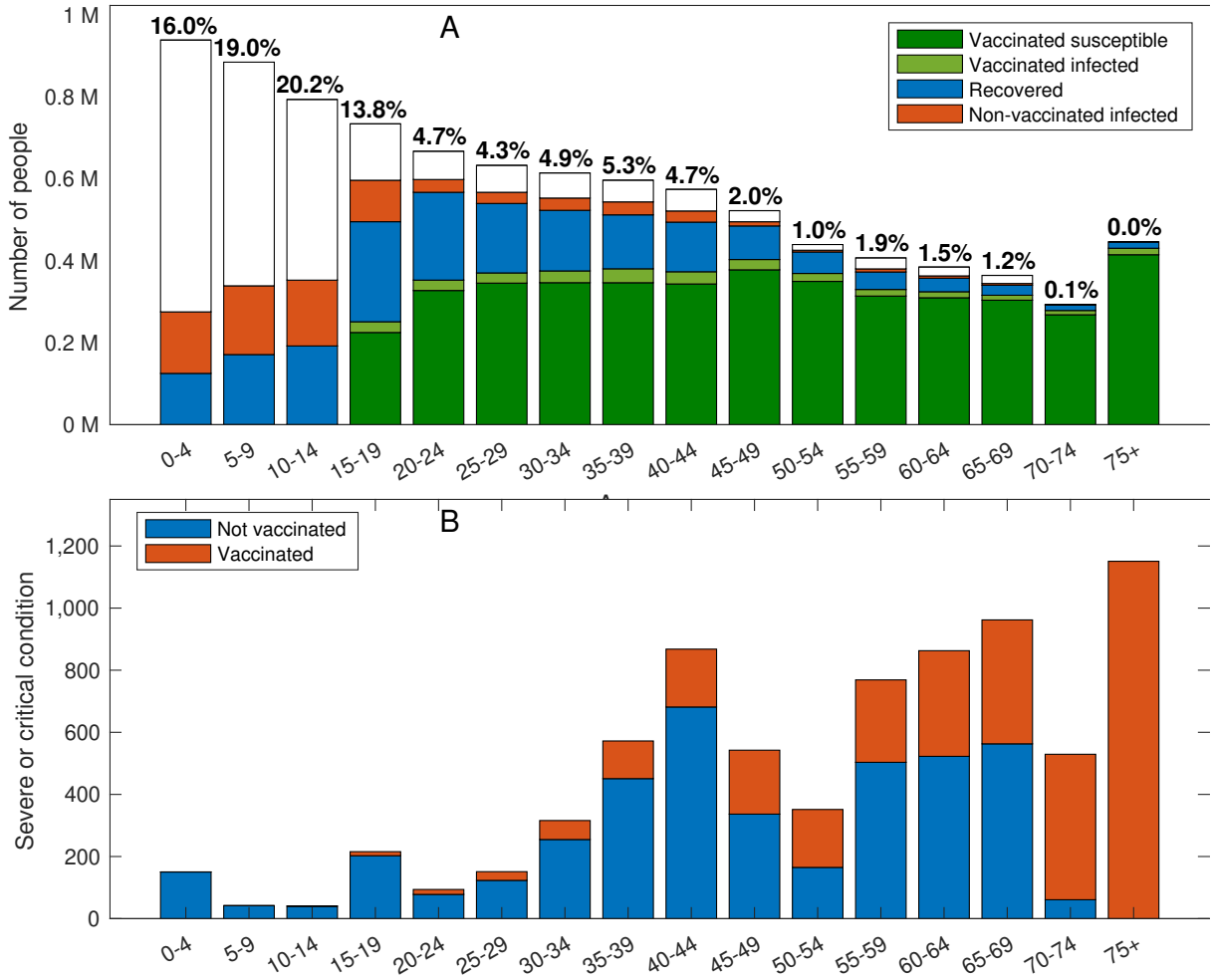

Figure 23: **Final size of epidemic: Israel (updated: mid April 2021).** A: The expected outcome when the basic reproduction number is $R_0 = 3$ using the real data of the vaccination campaign and the known cases in Israel. Particularly, the vaccination campaign covers 55% of the population, and overall 74% of the population is vaccinated or recovered. Vaccine eligibility is limited to ages 16 and above. The text corresponds to the percent of non-vaccinated infected individuals in each age group. B: Distribution of severe cases among age groups, and among vaccinated and non-vaccinated populations.

came voluntary and school system operation has been fully restored, but the impact of these changes on R_0 are yet unknown. We now compute the outcomes in a scenario of $R_0 = 3$. Our computation shows an overall infection of 0.76 million people (8.1% of the population), and

the additional mortality of 1400 people (150 people per 1 million), see Figure 23A. We further consider the distribution of severe or critical cases among vaccinated and non-vaccinated, and observe that in this case roughly 45% of the severe cases are vaccinated, see Figure 23B. This result is due to partial vaccine efficacy, i.e., the assumption of 80% vaccine efficacy in preventing infections and overall 95% vaccine efficacy in preventing severe disease. This emphasizes the need to maintain preventive measures in high-risk population, and also the importance of indirect protection.

We further find that additional vaccination of 90% of age group 12-15 (vaccination of roughly 420,000 people) increases the estimated basic reproduction number at which Israel achieves herd immunity from $R_0 \approx 2.6$ to $R_0 \approx 2.9$. In this case, overall outcomes in the scenario of $R_0 = 3$ are reduced to roughly a third of the expected outcomes without vaccination of age group 12-15, e.g., infection reduces from 0.76 million to 0.25 million people and mortality reduces from 1400 to 500.

One can also consider the optimal allocation of additional vaccines, namely if an additional supply of vaccines becomes available - how should they be allocated to different age groups? To answer this question, we compute the Pareto front of outcomes resulting from an additional supply of vaccines when $R_0 = 3.5$[1]. We do not allow, however, additional allocation of vaccines to those 70 and older since vaccine converge in this age group is nearly maximized at this stage. We find that the Pareto front nearly collapsed to a point corresponding to an optimal allocation of half a million vaccines which allocates roughly 200,000 vaccines to age groups $15 - 19$ (30% of age group) and the vast majority of the rest in age group $35 - 39$. In particular, under the assumption that the contact structure and relative susceptibility is uniform within each age group, this allocation can be realized by allocating 200,000 vaccines to age groups $16 - 19$. Therefore, under current assumptions, the optimal allocation for the scenario considered here

[1] We do not consider $R_0 = 3$ as in the previous example since at this value of R_0 herd immunity can be achieved with the additional supply of vaccines

does not include the vaccination of those under 16. This stems from the assumptions that the relative susceptibility and infectivity of children under the age of 16 is lower than that of older ages, and the estimate that about 24% of age group 10-15 is recovered and fully immune to re-infections. We further observe that the minimal number of infections is considerable, and spans roughly 20% of the age group 0-15. The number of infections can be further decreased by increasing vaccine coverage. Even more than in all other cases presented in this work, the homogeneous allocation, as well as the vast majority of random allocations, give rise to outcomes that are significantly worse than those that arise from allocations along the Pareto front. This is stems from the fact that the outcomes are strongly influenced by infections of vaccinated elderly populations, i.e., allocation of vaccines to age-groups whom their vast are already see Figure 23B. This implies that, at this stage, precision in implementing the optimal allocation is important, and that it is necessary to re-evaluate the optimal allocations as the vaccination effort continues.

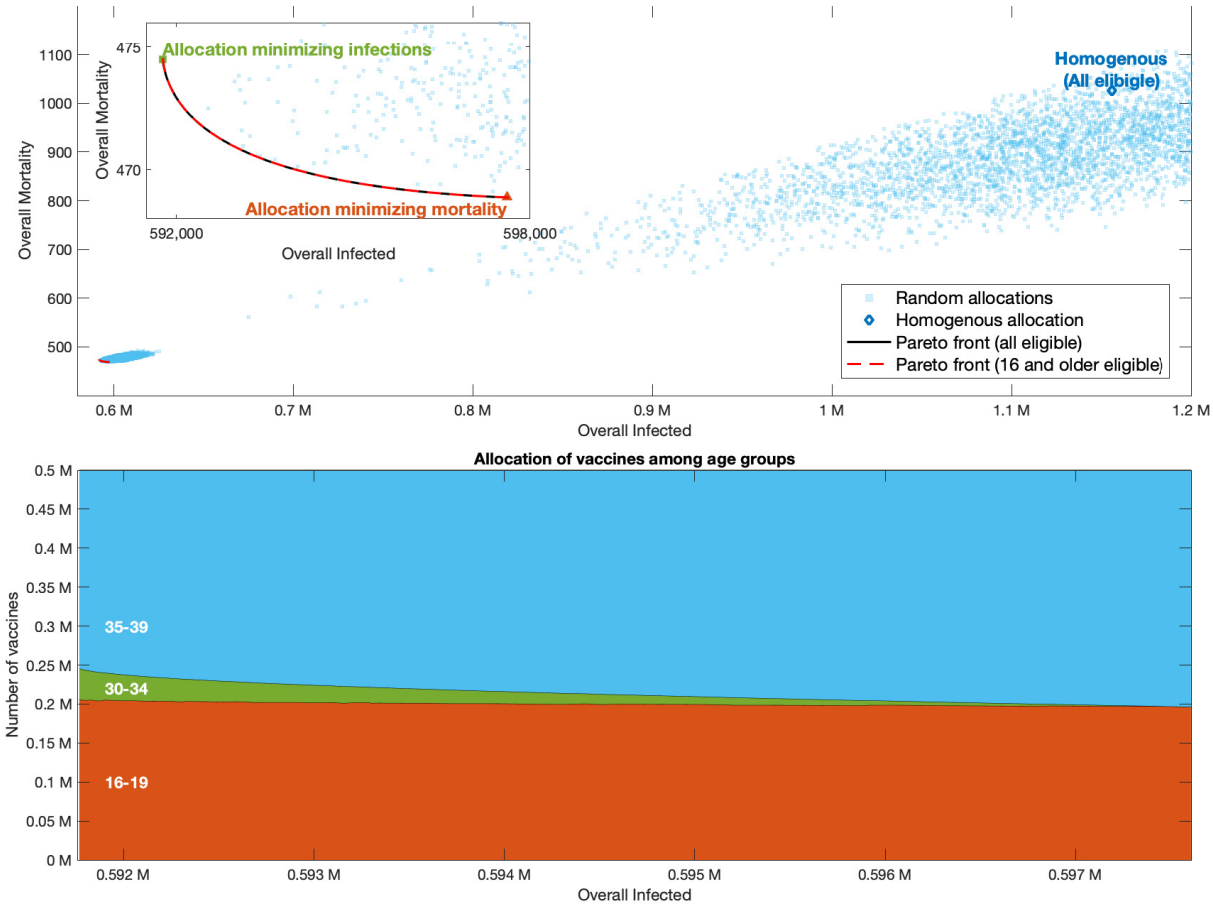

Figure 24: **Pareto front - vaccination of an additional half a million people in Israel.** Top graph presents outcomes of random allocation when all ages are eligible for vaccination (square blue markers). Black solid is the Pareto front when all ages are eligible for vaccination. This front coincides with the Pareto fronts in the cases when vaccine eligibility is limited to ages 12 and older or to ages 16 and older. The sub-graph zooms in on the Pareto front. Bottom Graphs: Vaccine allocations along the corresponding Pareto fronts when all ages are eligible for vaccination. The information presented in this graph is smoothed by considering the convex hull of the Pareto curve.